Statistical Inference for High-Dimensional Spectral Density Matrix

Jinyuan Chang, Qing Jiang, Tucker McElroy & Xiaofeng Shao

View supplementary material ⧉

Published online: 25 Apr 2025.

Submit your article to this journal ⧉

View related articles ⧉

View Crossmark data ⧉

Taylor & Francis
Taylor & Francis Group

Check for updates

Statistical Inference for High-Dimensional Spectral Density Matrix

Jinyuan Chang[a,b,c] (ID), Qing Jiang[d], Tucker McElroy[e], and Xiaofeng Shao[f]

[a]Joint Laboratory of Data Science and Business Intelligence, Southwestern University of Finance and Economics, Chengdu, Sichuan, China; [b]Big Data Laboratory on Financial Security and Behavior (MOE Philosophy and Social Sciences Laboratory), Southwestern University of Finance and Economics, Chengdu, Sichuan, China; [c]Academy of Mathematics and Systems Science, Chinese Academy of Sciences, Beijing, China; [d]Faculty of Arts and Sciences, Beijing Normal University, Zhuhai, China; [e]Research and Methodology Directorate, U.S. Census Bureau, Washington, DC; [f]Department of Statistics and Data Science, and Department of Economics, Washington University in St Louis, St. Louis, MO

ABSTRACT

The spectral density matrix is a fundamental object of interest in time series analysis, and it encodes both contemporary and dynamic linear relationships between component processes of the multivariate system. In this article we develop novel inference procedures for the spectral density matrix in the high-dimensional setting. Specifically, we introduce a new global testing procedure to test the nullity of the cross-spectral density for a given set of frequencies and across pairs of component indices. For the first time, both Gaussian approximation and parametric bootstrap methodologies are employed to conduct inference for a high-dimensional parameter formulated in the frequency domain, and new technical tools are developed to provide asymptotic guarantees of the size accuracy and power for global testing. We further propose a multiple testing procedure for simultaneously testing the nullity of the cross-spectral density at a given set of frequencies. The method is shown to control the false discovery rate. Both numerical simulations and a real data illustration demonstrate the usefulness of the proposed testing methods. Supplementary materials for this article are available online, including a standardized description of the materials available for reproducing the work.

1. Introduction

The spectral density matrix plays an important role in time series analysis, as it completely characterizes the second order properties of a multivariate stationary time series; moreover, it is a crucial quantity in the modeling, inference, and prediction of time series. It has been used in discriminant analysis for time series (Taniguchi and Kakizawa 2000), identification and estimation of generalized dynamic factor models (Forni et al. 2000), and non-correlation/independence testing for two time series (Eichler 2007; Shao 2009), to name a few examples. Estimation and inference for the univariate spectral density and multivariate low-dimensional spectral density matrix have a long history, and classical methods based on the smoothed periodogram or lag-window estimates have been well documented in classical textbooks such as Hannan (1970), Priestley (1981), Brillinger (2001), and Brockwell and Davis (2006). More recent contributions can be found in Shao and Wu (2007), Liu and Wu (2009), and Wu and Zaffaroni (2018), among others.

With the advancement of science and technology, high-dimensional time series have been increasingly collected in many areas, such as neuroimaging studies, finance, and climate science, as well as official statistics. This situation motivates the development of new statistical methodology and theory to accommodate the data's high dimensionality. For example, the classical smoothed periodogram estimate

of the multivariate spectral density matrix can be improved by a shrinkage approach; see Böhm and von Sachs (2008, 2009), Fiecas and Ombao (2011), and Fiecas and von Sachs (2014), among others. The popular regularization approaches used in covariance and precision matrix estimation, such as graphical LASSO (Yuan and Lin 2007), thresholding (Bickel and Levina 2008), and constrained L_1 minimization (Cai, Liu, and Luo 2011), have been extended to estimate either the high-dimensional spectral density matrix or its inverse by Sun et al. (2018), Fiecas et al. (2019), and Tugnait (2022). Related work along this line also includes Zhang and Wu (2021), which established convergence rates of regularized estimates of the spectral density matrix and its inverse under a high-dimensional locally stationary framework. Recently, Barigozzi and Farne (2024) introduced a new estimator of the high-dimensional spectral density matrix—under the assumptions of low rank and sparse structure—via minimizing a quadratic loss under a nuclear norm, together with a L_1 norm constraint to control the latent rank and residual sparsity pattern.

While the literature on estimating the high-dimensional spectral density matrix or its inverse has been growing rapidly, there seems to be relatively less work devoted to inference for the spectral density matrix, which is our focus here. In this article, we aim to develop new theory and methods for the inference of the spectral density matrix of a high-dimensional

weakly stationary time series. In particular, we propose a new maximum-type test statistic to test for the joint hypothesis that the cross-spectral density is zero for a given set of frequencies and pairs of indices. We establish a Gaussian approximation result for our maximum-type test statistic, and provide a computationally feasible parametric bootstrap-based approach to approximate its finite sample distribution. Building on the newly established theory, we further develop a multiple testing procedure to recover the support of the spectral density matrix for a given set of frequencies.

Since the seminal work of Chernozhukov, Chetverikov, and Kato (2013), the technique of Gaussian approximation has undergone rapid developments; see Chernozhukov, Chetverikov, and Kato (2017, 2019), Chen (2018), Chen and Kato (2019), Fang and Koike (2020), and Chernozhukov et al. (2022), among others. A recent review of high-dimensional data bootstrap and Gaussian approximation is provided by Chernozhukov et al. (2023). The extension of Gaussian approximation to high-dimensional time series was first developed by Zhang and Wu (2017) and Zhang and Cheng (2018), but their focus was mainly on inference for quantities such as means and autocovariance matrices, which are formulated in the time domain. By contrast, our parameter of interest is the cross-spectral density measured over a set of frequencies, and our technical treatment is rather different from that of Zhang and Wu (2017) and Zhang and Cheng (2018). The closest works to our article, from a technical perspective, are Chang, Jiang, and Shao (2023) and Chang, Chen, and Wu (2024a).

Let $\{\mathbf{x}_t\}$ be a p-dimensional weakly stationary time series. Denote by $\mathbf{F}(\omega) = \{f_{i,j}(\omega)\}_{p \times p} \in \mathbb{C}^{p \times p}$ the spectral density matrix of $\{\mathbf{x}_t\}$ at frequency $\omega \in [-\pi, \pi)$. Our main goal in this article is to establish the Gaussian approximation to the distribution of

$$\mathcal{T} = \sup_{\omega \in \mathcal{J}} \max_{(i,j) \in \mathcal{I}} \left| \sqrt{\frac{n}{l_n}} \{\hat{f}_{i,j}(\omega) - f_{i,j}(\omega)\} \right|^2, \quad (1)$$

where $\mathcal{I} \subset \{1, \ldots, p\}^2$, $\mathcal{J} \subset [-\pi, \pi)$, and $\hat{f}_{i,j}(\omega)$ is some kernel-based estimate of $f_{i,j}(\omega)$ with bandwidth l_n. Such a Gaussian approximation result provides a technical tool for the inference of the high-dimensional spectral density matrix. For each given $(i,j) \in \mathcal{I}$ and $\omega \in \mathcal{J}$, $|\sqrt{n/l_n}\{\hat{f}_{i,j}(\omega) - f_{i,j}(\omega)\}|^2$ usually converges in distribution to the sum of squares of two correlated normal random variables. Our setting is quite different from those considered in existing works, and this generates several technical challenges for establishing the Gaussian approximation to the distribution of $\mathcal{T}$. See our detailed discussion in Remark 1(d) in Section 2.2. In addition, we apply our Gaussian approximation results to obtain false discovery rate (FDR) control in the multiple testing procedure, which not only expands the application of our Gaussian approximation results, but also extends the validity of FDR control to the high-dimensional time series setting.

As we mentioned earlier, the literature on the inference for the high-dimensional spectral density matrix is scarce, and we are only aware of two recent papers. Motivated by testing the mutual independence of the component series in a p-dimensional complex-valued Gaussian time series, Loubaton, Rosuel, and

Vallet (2023) investigated the asymptotic distribution for the maximum of smoothing-based estimators of the coherence (the standarized cross-spectral density), and showed that its null-distribution converges to a Gumbel limiting distribution when $p/n = o(1)$, as well as some other conditions on the smoothing span. Krampe and Paparoditis (2022) developed new statistical inference procedures for coherences and partial coherences of a p-dimensional real-valued time series. They addressed the estimation of partial coherence using a debiased approach, and developed a testing procedure for the null hypothesis that the partial coherences do not exceed some user-specified threshold value within a frequency band of interest. When $p = o(n^\tau)$ for some constant $\tau > 0$, they showed that the limiting distribution for the maximum of sample partial coherence over frequencies is the classical Gumbel distribution (or its variant).

In contrast to these two works, we focus on the Gaussian approximation to the distribution of $\mathcal{T}$ defined as (1), which can also be used to conduct inference for coherences (see Section 2.1 for details). It is worth noting that the maximum-type test statistics in both Loubaton, Rosuel, and Vallet (2023) and Krampe and Paparoditis (2022) are taken over a set of frequencies that are equally spaced, with the spacing having larger order of magnitude than $2\pi/n$ (the spacing for consecutive Fourier frequencies). This construction appears to be necessary in order for these authors to obtain a Gumbel limiting distribution. Technically speaking, the derivation of the Gumbel limiting distribution relies on the weak dependency among test statistics across frequencies. Hence, in Loubaton, Rosuel, and Vallet (2023) and Krampe and Paparoditis (2022), the spacing between the frequencies cannot be too close. In addition, Loubaton, Rosuel, and Vallet (2023) required the time series to be mean-zero stationary and complex-valued Gaussian time series with mutually independent component time series under the null. By contrast, we allow some dependence between different components of time series under the null, and we consider real-valued time series in this article. Our proposed method can also be extended to complex-valued time series but is not pursued here. Krampe and Paparoditis (2022) mainly focused on the hypothesis testing and support recovery of the partial coherence matrix of real-valued high-dimensional time series. From the viewpoint of asymptotic approximation, it is a common belief that the maximum-type statistics usually converge slowly to the Gumbel distributions (Hall 1991), and the bootstrap is often employed to provide a better finite sample approximation. By contrast, our Gaussian approximation theory does not require any dependence structure among the quantities $|\sqrt{n/l_n}\{\hat{f}_{i,j}(\omega) - f_{i,j}(\omega)\}|^2$ across frequencies, so we have no requirements on the spacing of frequencies $\omega \in \mathcal{J}$ as long as they are distinct and fall into $[-\pi, \pi)$. Notice that the limiting distribution of $\mathcal{T}$ defined in (1) may not admit a closed form (or even does not exist), but its finite sample distribution can nevertheless be well-approximated by its parametric bootstrap counterpart. The technical tools employed in these two papers and ours are very different.

A primary application of our inference procedure for the high-dimensional spectral density matrix is the division of large time series databases into batches suitable for joint analysis.

For example, a database of county-level time series can be organized into batches by state, and it is of interest to know if there is significant content in the cross-spectra of two batches; if so, there may be merit in jointly modeling the batches, but otherwise analysis can proceed upon smaller collections. A second motivation for our work comes from the processing and analysis of seasonal time series at statistical agencies such as the U.S. Census Bureau (USCB). At USCB, many weekly, monthly, and quarterly economic time series are published, all of which exhibit seasonality of varying types and degrees. The USCB performs seasonal adjustment of such time series in order to remove seasonality; both the original and seasonally adjusted data are published for public use. Seasonal adjustment is a vast world-wide undertaking, with the statistical agencies of all developed countries (as well as many private companies) adjusting thousands or millions of time series every month (or quarter). One important task in practice is to evaluate the effectiveness of seasonal adjustment, that is, whether the strong seasonality has been properly removed or whether there is an issue of over-adjustment (McElroy 2021; McElroy and Roy 2022). For example, seasonal adjustment methods that are intended to remove seasonality sometimes—when applied to a time series with weak seasonality—result in zero power spectrum at a "seasonal frequency", for example, $f_{i,i}(\pi/2) = 0$ for a quarterly time series. This motivates a joint testing problem over many time series, where we wish to identify which series have zero power at the seasonal frequencies (i.e., have been over-adjusted).

The rest of the article is organized as follows. Section 2 presents the spectral density matrix estimate, a general Gaussian approximation procedure, and the related theory. Section 3 contains two applications, including global testing and support recovery via a multiple testing procedure. Section 4 investigates the finite sample performance of the proposed testing procedures via numerical simulation, and Section 5 provides an illustration based on county-level quarterly time series of new hires. Section 6 concludes the article. All technical details are relegated to the supplementary material. For practical convenience we have developed—in the R package HDTSA (Chang et al. 2024c)—two R-functions `SpecTest` and `SpecMulTest` that implement the global testing and the multiple testing procedures in an automatic manner, respectively.

Notation. Denote by $I(\cdot)$ the indicator function. For any positive integer $q \geq 2$, we write $[q] = \{1, \ldots, q\}$, and let $[q]^2 = [q] \times [q]$ denote the Cartesian product of $[q]$. Let $|\mathcal{F}|$ be the cardinality of a countable set $\mathcal{F}$. For two positive real-valued sequences $\{a_n\}$ and $\{b_n\}$, we write $a_n \lesssim b_n$ if $\limsup_{n\to\infty} a_n/b_n \leq c_0$ for some positive constant c_0, $a_n \asymp b_n$ if $a_n \lesssim b_n$ and $b_n \lesssim a_n$ hold simultaneously, and $a_n \ll b_n$ if $\limsup_{n\to\infty} a_n/b_n = 0$. For a complex-valued number x, denote by $|x|$ its modulus. The operator $\otimes$ denotes the Kronecker product. For any real-valued numbers x and y, we write $|x|_+ = \max(0, x)$ and $x \vee y = \max(x, y)$. Denote by $\mathbb{S}^{q-1}$ the q-dimensional unit sphere. For a q-dimensional vector $\mathbf{a}$, denote by $\mathbf{a}_{\mathcal{L}}$ the subvector of $\mathbf{a}$ consisting of the components indexed by a given index set $\mathcal{L} \subset [q]$. For any $q_1 \times q_2$ matrix $\mathbf{M} = (m_{i,j})_{q_1 \times q_2}$, let $|\mathbf{M}|_\infty = \max_{i \in [q_1], j \in [q_2]} |m_{i,j}|$. Let $\mathbf{1}_d$ and $\mathbf{I}_d$ be, respectively, a d-dimensional vector with all components being 1, and a $d \times d$ identity matrix.

2. Some Technical Results

2.1. Preliminary

Let $\mathbf{x}_t = (x_{1,t}, \ldots, x_{p,t})^\top$ be a p-dimensional weakly stationary time series with mean vector $\boldsymbol{\mu} = \mathbb{E}(\mathbf{x}_t)$ and autocovariance matrix $\boldsymbol{\Gamma}(k) \equiv \{\gamma_{i,j}(k)\}_{p \times p} = \text{cov}(\mathbf{x}_{t+k}, \mathbf{x}_t)$. When $\sum_{k=-\infty}^\infty |\gamma_{i,j}(k)| < \infty$ for each $i, j \in [p]$, we can define the spectral density matrix $\mathbf{F}(\omega)$ for $\omega \in [-\pi, \pi)$ as

$$\mathbf{F}(\omega) \equiv \{f_{i,j}(\omega)\}_{p \times p} = \frac{1}{2\pi} \sum_{k=-\infty}^\infty \boldsymbol{\Gamma}(k) e^{-\iota k \omega},$$

where $\iota = \sqrt{-1}$. Given the observations $\mathcal{X}_n = \{\mathbf{x}_1, \ldots, \mathbf{x}_n\}$, we can estimate $\mathbf{F}(\omega)$ by

$$\widehat{\mathbf{F}}(\omega) \equiv \{\hat{f}_{i,j}(\omega)\}_{p \times p} = \frac{1}{2\pi} \sum_{k=-l_n}^{l_n} \mathcal{W}\left(\frac{k}{l_n}\right) \widehat{\boldsymbol{\Gamma}}(k) e^{-\iota k \omega}, \quad (2)$$

where $\mathcal{W}(\cdot)$ is a symmetric kernel function, $l_n = o(n)$ is the bandwidth, and

$$\widehat{\boldsymbol{\Gamma}}(k) = \frac{1}{n} \sum_{t=\max(1, -k+1)}^{\min(n, n-k)} (\mathbf{x}_{t+k} - \bar{\mathbf{x}})(\mathbf{x}_t - \bar{\mathbf{x}})^\top \quad (3)$$

with $\bar{\mathbf{x}} = n^{-1} \sum_{t=1}^n \mathbf{x}_t$. To reduce the bias involved in (2), for some constant $c \in (0, 1]$, we adopt the flat-top kernel suggested by Politis (2011):

$$\mathcal{W}(u) = I(|u| \leq c) + \frac{|u| - 1}{c - 1} I(c < |u| \leq 1). \quad (4)$$

For given $(i, j) \in [p]^2$ and $i < j$, define the coherence spectrum at frequency ω by

$$\text{coh}_{i,j}(\omega) = \frac{f_{i,j}(\omega)}{\{f_{i,i}(\omega) f_{j,j}(\omega)\}^{1/2}}.$$

As mentioned in Priestley (1981), the coherence may be interpreted as the correlation coefficient between the random coefficients in the spectral representations of the components in $x_{i,t}$ and $x_{j,t}$ at frequency ω. Thus, $\text{coh}_{i,j}(\omega) = 0$ for all $\omega \in [-\pi, \pi)$ is equivalent to $f_{i,j}(\omega) = 0$ for all $\omega \in [-\pi, \pi)$, which implies the two processes $\{x_{i,t}\}$ and $\{x_{j,t}\}$ are linearly unrelated at all lags. Within the scope of linear time series models, the joint modeling of $\{(x_{i,t}, x_{j,t})\}$ can be simplified by modeling the linear serial dependence of $\{x_{i,t}\}$ and $\{x_{j,t}\}$ separately, provided that $\max_{\omega \in [-\pi, \pi)} |f_{i,j}(\omega)| = 0$. For a p-dimensional weakly stationary time series $\{\mathbf{x}_t\}$, it is thus of great importance to recover the support of nonzero coherence, that is,

$$\mathscr{S}_f := \left\{ (i, j) \in [p]^2 \setminus \{(1,1), \ldots, (p,p)\} : \right.$$

$$\left. \max_{\omega \in [-\pi, \pi)} |f_{i,j}(\omega)| \neq 0 \right\}. \quad (5)$$

It is worth noting that the coherence also plays an important role in characterizing the functional connectivity between neural

regions within the brain based on functional magnetic resonance imaging data; see Sun, Miller, and D'Esposito (2004) and Bowyer (2016). Additionally, in terms of joint modeling in the frequency domain, it is of interest to understand the behavior of the cross-spectrum (or coherence) for a specific set of frequencies. For example, for a quarterly time series, we are interested in the coherence at the "seasonal frequency" $\pi/2$ and the "trend frequency" 0; if joint modeling of low-frequency fluctuation is of particular interest, we may want to focus on a pre-specified frequency interval such as $[-\omega_0, \omega_0]$, where ω_0 is determined by the user based on the characteristics of time series, such as sample size and expected seasonal behavior (e.g., monthly or quarterly). For the application of seasonal over-adjustment mentioned in Section 1, we also wish to consider the joint testing problem $H_0 : f_{i,i}(\omega_0) = 0$ for all $i \in [p]$, and the recovery of the support of indices that correspond to nonzero power auto-spectrum at ω_0, where $\omega_0 \in \{-\pi, -\pi/2, 0, \pi/2\}$.

To study the above-mentioned testing and support recovery problems, we define

$$T_n(\omega; \mathcal{I}) = \max_{(i,j) \in \mathcal{I}} \left| \sqrt{\frac{n}{l_n}} \{\hat{f}_{i,j}(\omega) - f_{i,j}(\omega)\} \right|^2$$

for a given index set $\mathcal{I} \subset [p]^2$ and $\omega \in [-\pi, \pi)$. Given a subset $\mathcal{J} \subset [-\pi, \pi)$, we will first establish in Section 2.2 the Gaussian approximation to the distribution of $\sup_{\omega \in \mathcal{J}} T_n(\omega; \mathcal{I})$. In practical problems, we mainly focus on two kinds of configurations for $\mathcal{J}$, viz. (a) $\mathcal{J} = \{\omega_1, \ldots, \omega_K\}$ is a set with K distinct frequencies $-\pi \leq \omega_1 < \omega_2 < \cdots < \omega_K < \pi$, where K may grow with the sample size n; (b) $\mathcal{J} = [\omega_L, \omega_U]$ is an interval with $-\pi \leq \omega_L < \omega_U \leq \pi$, where $\mathcal{J} = [\omega_L, \pi)$ if $\omega_U = \pi$. Based on the established Gaussian approximation theory, we can address the following inference problems of a high-dimensional time series:

- (Global hypothesis testing). For given $\mathcal{I}$ and $\mathcal{J}$, consider the testing problem $H_0 : f_{i,j}(\omega) = 0$ for any $(i,j) \in \mathcal{I}$ and $\omega \in \mathcal{J}$ versus $H_1 : H_0$ is not true. Here $\mathcal{I}$ and $\mathcal{J}$ can be chosen according to the user's interest. If we are interested in simultaneously testing the zero power auto-spectrum at a seasonal frequency $\omega_0 \in \{-\pi, -\pi/2, 0, \pi/2\}$, we can select $\mathcal{I} = \{(1,1), \ldots, (p,p)\}$ and $\mathcal{J} = \{\omega_0\}$. If testing for the zero cross-spectrum at all frequencies is of interest, we can set $\mathcal{I} = [p]^2 \setminus \{(1,1), \ldots, (p,p)\}$ and $\mathcal{J} = [-\pi, \pi)$. See Section 3.1 for details.
- (Support recovery). In the event that the global null is rejected, we are interested in the support of nonzero elements, that is, $\{(i,j) \in \mathcal{I} : \sup_{\omega \in \mathcal{J}} |f_{i,j}(\omega)| \neq 0\}$. For example, to recover $\mathscr{S}_f$ defined as (5), we can consider a multiple testing problem with $(p^2 - p)/2$ marginal hypotheses $H_{0,i,j} : \max_{\omega \in [-\pi,\pi)} |f_{i,j}(\omega)| = 0$ versus $H_{1,i,j} : \max_{\omega \in [-\pi,\pi)} |f_{i,j}(\omega)| \neq 0$, with $(i,j) \in [p]^2$ and $i < j$. For each given (i,j), we can obtain the p-value for the marginal null hypothesis $H_{0,i,j}$ by our established Gaussian approximation result for the distribution of $\sup_{\omega \in \mathcal{J}} T_n(\omega; \mathcal{I})$ with selecting $\mathcal{I} = \{(i,j)\}$ and $\mathcal{J} = [-\pi, \pi)$. Based on the $(p^2 - p)/2$ obtained p-values, we can propose a FDR control procedure to estimate $\mathscr{S}_f$ as in (5). See Section 3.2 for details.

2.2. A General Gaussian Approximation Procedure

Write $r = |\mathcal{I}|$, $\tilde{n} = n - 2l_n$, $\mathbf{\Gamma}(k) \equiv \{\gamma_{i,j}(k)\}_{p \times p}$ and $\widehat{\mathbf{\Gamma}}(k) \equiv \{\hat{\gamma}_{i,j}(k)\}_{p \times p}$. Define $\mathring{\mathbf{x}}_t \equiv (\mathring{x}_{1,t}, \ldots, \mathring{x}_{p,t})^\top = \mathbf{x}_t - \boldsymbol{\mu}$ for any $t \in [n]$. Let $\boldsymbol{\chi}(\cdot) = \{\chi_1(\cdot), \chi_2(\cdot)\}$ be a given bijective mapping from $[r]$ to $\mathcal{I}$ such that for any $(i,j) \in \mathcal{I}$, there exists a unique $\ell \in [r]$ satisfying $(i,j) = \boldsymbol{\chi}(\ell)$. For each $t \in [\tilde{n}]$ and $\ell \in [r]$, we define a $(2l_n + 1)$-dimensional vector

$$\mathbf{c}_{\ell,t} = \frac{1}{2\pi} \{\mathring{x}_{\chi_1(\ell),t} \mathring{x}_{\chi_2(\ell),t+l_n} - \gamma_{\boldsymbol{\chi}(\ell)}(-l_n), \ldots,$$
$$\mathring{x}_{\chi_1(\ell),t+2l_n} \mathring{x}_{\chi_2(\ell),t+l_n} - \gamma_{\boldsymbol{\chi}(\ell)}(l_n)\}^\top. \qquad (6)$$

Notice that $\mathbb{E}(\mathbf{c}_{\ell,t}) = \mathbf{0}$. Let $\mathbf{c}_t = (\mathbf{c}_{1,t}^\top, \ldots, \mathbf{c}_{r,t}^\top)^\top$ with $\mathbf{c}_{\ell,t}$ defined in (6). Define

$$\check{\boldsymbol{\eta}}^{\text{ext}}(\omega) \equiv \{\check{\eta}_1^{\text{ext}}(\omega), \ldots, \check{\eta}_{2r}^{\text{ext}}(\omega)\}^\top$$

$$= \{\mathbf{I}_r \otimes \mathbf{A}(\omega)\} \frac{1}{\sqrt{n}} \sum_{t=1}^{\tilde{n}} \mathbf{c}_t, \qquad (7)$$

where

$$\mathbf{A}(\omega) = \frac{1}{\sqrt{l_n}} \begin{pmatrix} \cos(-l_n\omega) & \cdots & \cos(l_n\omega) \\ -\sin(-l_n\omega) & \cdots & -\sin(l_n\omega) \end{pmatrix}$$
$$\times \text{diag}\{\mathcal{W}(-l_n/l_n), \ldots, \mathcal{W}(l_n/l_n)\}. \qquad (8)$$

Denote the long-run covariance of the sequence $\{\mathbf{c}_t\}_{t=1}^{\tilde{n}}$ by

$$\mathbf{\Xi} = \text{Var}\left(\frac{1}{\sqrt{\tilde{n}}} \sum_{t=1}^{\tilde{n}} \mathbf{c}_t\right). \qquad (9)$$

For any $\omega_1, \omega_2 \in [-\pi, \pi)$, we define

$$\mathbf{\Sigma}(\omega_1, \omega_2) = \{\mathbf{I}_r \otimes \mathbf{A}(\omega_1)\} \mathbf{\Xi} \{\mathbf{I}_r \otimes \mathbf{A}^\top(\omega_2)\}. \qquad (10)$$

Then $\text{cov}\{\check{\boldsymbol{\eta}}^{\text{ext}}(\omega_1), \check{\boldsymbol{\eta}}^{\text{ext}}(\omega_2)\} = (\tilde{n}/n)\mathbf{\Sigma}(\omega_1, \omega_2)$ for any $\omega_1, \omega_2 \in [-\pi, \pi)$ with $\check{\boldsymbol{\eta}}^{\text{ext}}(\omega)$ defined as (7). To investigate the limiting distribution of $\sup_{\omega \in \mathcal{J}} T_n(\omega; \mathcal{I})$, we need the following regularity conditions. The validity of these conditions are discussed in Section A of the supplementary material.

Condition 1. There exist some universal constants $C_1 > 0$ and $C_2 > 1$ such that $\mathbb{E}\{\exp(C_1|x_{j,t}|^2)\} \leq C_2$ for any $t \in [n]$ and $j \in [p]$.

Condition 2. Let $\mathcal{F}_{-\infty}^u$ and $\mathcal{F}_{u+k}^{+\infty}$ be the σ-fields generated, respectively, by $\{\mathbf{x}_t\}_{t \leq u}$ and $\{\mathbf{x}_t\}_{t \geq u+k}$. Define

$$\alpha_n(k) := \sup_t \sup_{(A,B) \in \mathcal{F}_{-\infty}^t \times \mathcal{F}_{t+k}^{+\infty}} |\mathbb{P}(A \cap B) - \mathbb{P}(A)\mathbb{P}(B)|.$$

There exist some universal constants $C_3 > 0$ and $C_4 > 0$ such that $\alpha_n(k) \leq C_3 \exp(-C_4 k)$ for any positive k.

Condition 3. There exists a universal constant $C_5 > 0$ such that $\inf_{\omega \in \mathcal{J}} \mathbf{d}^\top \mathbf{\Sigma}(\omega, \omega) \mathbf{d} \geq C_5$ for any $\mathbf{d} \in \bigcup_{j=1}^r \{\mathbf{d} \in \mathbb{S}^{2r-1} : \mathbf{d}_{S_j} \in \mathbb{S}^1\}$ with $S_j = \{2j-1, 2j\}$.

Notice that in these conditions there are no explicit requirements on the cross-series dependence, and both weak and strong cross-series dependence are allowed by our theory. In particular, the marginal covariance matrix can be banded or AR(1)-type, representing weak cross-series dependence. Or it can be a compound symmetric matrix, which implies strong cross-series dependence. As a result, we can establish the following Gaussian approximation result.

Proposition 1. Assume $r \geq n^{\kappa}$ for some sufficiently small constant $\kappa > 0$, and let Conditions 1–3 hold. As $n \to \infty$, the following two assertions are valid.

(i) If $\mathcal{J} = \{\omega_1, \ldots, \omega_K\}$ and $\log(Kr) \ll n^{1/9} l_n^{-1} \log^{-8/3}(l_n)$, with the bandwidth l_n in (2) satisfying $l_n \log^{8/3}(l_n) \ll n^{1/9}$ and $l_n \geq \max\{2, C \log(Kr)\}$ for some sufficiently large constant $C > 0$, then

$$\sup_{u \geq 0} \left| \mathbb{P}\left\{ \sup_{\omega \in \mathcal{J}} T_n(\omega; \mathcal{I}) \leq u \right\} - \mathbb{P}\left\{ \max_{j \in [Kr]} (s_{n,2j-1}^2 + s_{n,2j}^2) \leq u \right\} \right|$$

$$\lesssim \frac{l_n \log^{2/3}(l_n) \log(Kr)}{n^{1/9}}$$

for a $(2Kr)$-dimensional normally distributed random vector $\mathbf{s}_{n,\mathbf{y}} = (s_{n,1}, \ldots, s_{n,2Kr})^{\top} \sim \mathcal{N}(\mathbf{0}, \mathbf{H}\Xi\mathbf{H}^{\top})$, where $\mathbf{H} = \{\mathbf{I}_r \otimes \mathbf{A}^{\top}(\omega_1), \ldots, \mathbf{I}_r \otimes \mathbf{A}^{\top}(\omega_K)\}^{\top}$ with $\mathbf{A}(\omega)$ defined in (8), and Ξ is defined in (9).

(ii) If $\mathcal{J} = [\omega_L, \omega_U]$ and $\log r \ll n^{1/9} l_n^{-1} \log^{-8/3}(l_n)$, with the bandwidth l_n in (2) satisfying $l_n \log^{8/3}(l_n) \ll n^{1/9}$ and $l_n \geq \max(2, C \log r)$ for some sufficiently large constant $C > 0$, then

$$\sup_{u \geq 0} \left| \mathbb{P}\left\{ \sup_{\omega \in \mathcal{J}} T_n(\omega; \mathcal{I}) \leq u \right\} \right.$$

$$\left. - \mathbb{P}\left[\sup_{\omega \in \mathcal{J}} \max_{j \in [r]} \{g_{n,2j-1}^2(\omega) + g_{n,2j}^2(\omega)\} \leq u \right] \right|$$

$$\lesssim \frac{l_n \log^{2/3}(l_n) \log r}{n^{1/9}}$$

for a $(2r)$-dimensional Gaussian process $\mathbf{g}_n(\omega) = \{g_{n,1}(\omega), \ldots, g_{n,2r}(\omega)\}^{\top}$ with mean zero and covariance function $\Sigma(\omega_1, \omega_2)$ defined as (10).

Remark 1. (a) In Proposition 1 and other theoretical results of this article, we focus on the high-dimensional scenario by assuming $r \geq n^{\kappa}$ for some sufficiently small constant $\kappa > 0$. Such an assumption is quite mild in the literature of high-dimensional data analysis and it is not necessary for our theory, which is just used to simplify the presentation. In our theoretical proofs, we need to compare $\log n$ with $\log(Kr)$ or $\log r$ in many places. Without such a restriction, the proof of Proposition 1 will become much lengthier and some $\log(Kr)$ and $\log r$ terms in the theoretical results should be replaced by $\log(nKr)$ and $\log(nr)$, respectively. Our proposed Gaussian approximation procedure also works for the scenario with fixed r.

(b) If the bandwidth $l_n \asymp n^{\delta}$ for some constant $0 < \delta < 1/9$, then Proposition 1(i) holds provided that $\log(Kr) \ll \min\{n^{\delta}, n^{1/9-\delta} \log^{-8/3}(n)\}$, and Proposition 1(ii) holds provided that $\log r \ll \min\{n^{\delta}, n^{1/9-\delta} \log^{-8/3}(n)\}$.

(c) In practice, we can select the bandwidth l_n by adapting the simple rule suggested in Section 2.1 of Politis (2003). More specifically, let $l_n = 2\hat{m}$, where $\hat{m}$ is the smallest positive integer such that $p^{-2} \sum_{i=1}^{p} \sum_{j=1}^{p} |\hat{\rho}_{i,j}(\hat{m} + k)| < 2\sqrt{n^{-1} \log n}$ for $k = 1, \ldots, 5$, and $\hat{\boldsymbol{\rho}}(k) \equiv \{\hat{\rho}_{i,j}(k)\}_{p \times p} = \text{diag}\{\widehat{\boldsymbol{\Gamma}}(0)\}^{-1/2} \widehat{\boldsymbol{\Gamma}}(k) \text{diag}\{\widehat{\boldsymbol{\Gamma}}(0)\}^{-1/2}$ with $\widehat{\boldsymbol{\Gamma}}(k)$ specified in (3). Our numerical results in Section 4 verify its good finite-sample performance.

(d) Since $\{\mathbf{x}_t\}$ is an α-mixing sequence, we know $\{\mathbf{c}_t\}$ is also an α-mixing sequence. Denote by $\tilde{\alpha}_n(k)$ the α-mixing coefficient of the sequence $\{\mathbf{c}_t\}$. By Condition 2, it holds that $\tilde{\alpha}_n(k) \leq$

$\alpha_n(|k - 2l_n|_+) \leq C_3 \exp(-C_4 |k - 2l_n|_+)$. When l_n diverges with n, the α-mixing coefficients of the sequence $\{\mathbf{c}_t\}$ vary with n. For $\mathcal{J} = \{\omega_1, \ldots, \omega_K\}$, it is essential to establish the Gaussian approximation for $\mathbb{P}(n^{-1/2} \sum_{t=1}^{n-2l_n} \mathbf{H}\mathbf{c}_t \in A)$, where A is a 2-sparsely convex set, and $\mathbf{H}$ involves the frequency domain content. The most related works are Chang, Jiang, and Shao (2023) and Chang, Chen, and Wu (2024a). By comparison, Chang, Jiang, and Shao (2023) only considered the Gaussian approximation for hyperrectangle sets, not for sparsely convex sets, and the theoretical results for sparsely convex sets in Chang, Chen, and Wu (2024a) did not allow the α-mixing coefficients to vary with n. Therefore, the existing theoretical results cannot be applied to establish Proposition 1(i) when l_n diverges with n. For $\mathcal{J} = [\omega_L, \omega_U]$, we need to construct the Gaussian approximation for the distribution of the supremum of a stochastic process. The most related work is Chernozhukov, Chetverikov, and Kato (2014). With iid observations, they developed a new direct approach to approximate the supremum of general empirical processes by a sequence of supremums of Gaussian processes. However, our setting focuses on dependent observations and $\mathcal{T}$ is not the supremum of an empirical process. Hence, the results of Chernozhukov, Chetverikov, and Kato (2014) cannot be applied to our setting.

2.3. Parametric Bootstrap Procedure

To apply Proposition 1 to approximate the distribution of $\sup_{\omega \in \mathcal{J}} T_n(\omega; \mathcal{I})$, we need to propose an estimate of the long-run covariance Ξ given in (9). Recall $\widehat{\boldsymbol{\Gamma}}(k) = \{\hat{\gamma}_{i,j}(k)\}_{p \times p}$ and $\bar{\mathbf{x}} = (\bar{x}_1, \ldots, \bar{x}_p)^{\top} = n^{-1} \sum_{t=1}^{n} \mathbf{x}_t$. Let $\hat{\bar{\mathbf{x}}}_t = (\hat{\bar{x}}_{1,t}, \ldots, \hat{\bar{x}}_{p,t})^{\top} = \mathbf{x}_t - \bar{\mathbf{x}}$. For each $\ell \in [r]$, define a vector

$$\hat{\mathbf{c}}_{\ell,t} = \frac{1}{2\pi} \{ \hat{\bar{x}}_{\chi_1(\ell),t} \hat{\bar{x}}_{\chi_2(\ell),t+l_n} - \hat{\gamma}_{\chi(\ell)}(-l_n), \ldots, $$

$$\hat{\bar{x}}_{\chi_1(\ell),t+2l_n} \hat{\bar{x}}_{\chi_2(\ell),t+l_n} - \hat{\gamma}_{\chi(\ell)}(l_n) \}^{\top}, \quad (11)$$

which provides an approximation to $\mathbf{c}_{\ell,t}$ defined in (6). Write $\hat{\mathbf{c}}_t = (\hat{\mathbf{c}}_{1,t}^{\top}, \ldots, \hat{\mathbf{c}}_{r,t}^{\top})^{\top}$. Based on such defined $\hat{\mathbf{c}}_t$, we propose a kernel-type estimator suggested by Andrews (1991) for the long-run covariance matrix Ξ as follows:

$$\widehat{\boldsymbol{\Xi}} = \sum_{q=-\tilde{n}+1}^{\tilde{n}-1} \mathcal{K}\left(\frac{q}{b_n}\right) \widehat{\boldsymbol{\Pi}}(q), \quad (12)$$

where $\widehat{\boldsymbol{\Pi}}(q) = \tilde{n}^{-1} \sum_{t=\max(1,-q+1)}^{\min(\tilde{n},\tilde{n}-q)} \hat{\mathbf{c}}_{t+q} \hat{\mathbf{c}}_t^{\top}$, b_n is the bandwidth, and $\mathcal{K}(\cdot)$ is a symmetric kernel function. When r is fixed, Andrews (1991) systematically investigated the theoretical properties of such an estimator for the long-run covariance matrix, and showed that the Quadratic Spectral kernel $\mathcal{K}_{\text{QS}}(u) = 25/(12\pi^2 u^2)\{\sin(6\pi u/5)/(6\pi u/5) - \cos(6\pi u/5)\}$ is the optimal kernel in the sense of minimizing the asymptotic truncated mean square error. In our numerical work, we adopt this Quadratic Spectral kernel with the data-driven selected bandwidth suggested in Section 6 of Andrews (1991), that is, $b_n = 1.3221(\hat{a}\tilde{n})^{1/5}$, where $\hat{a} = \{\sum_{s=1}^{r(2l_n+1)} 4\hat{\rho}_s^2 \hat{\sigma}_s^4 (1 - \hat{\rho}_s)^{-8}\}/\{\sum_{s=1}^{r(2l_n+1)} \hat{\sigma}_s^4 (1 - \hat{\rho}_s)^{-4}\}$ with $\hat{\rho}_s$ and $\hat{\sigma}_s^2$ being, respectively, the estimated autoregressive coefficient and innovation variance from fitting an AR(1) model to time series

$\{\hat{c}_{s,t}\}_{t=1}^{\tilde{n}}$, the sth component sequence of $\{\hat{\mathbf{c}}_t\}_{t=1}^{\tilde{n}}$, where $\hat{\mathbf{c}}_t = \{\hat{c}_{1,t}, \ldots, \hat{c}_{r(2l_n+1),t}\}^\top$. Although Andrews' method is developed for low-dimensional data, both our theoretical and simulation results show that this estimator works reasonably well when r is large in relation to n. The performance of such kernel-type estimator with different kernels and choices of bandwidth has been studied in Chang, Jiang, and Shao (2023); their numerical results show that this method is robust for different kernels and bandwidths, and still works even in the high-dimensional case.

Condition 4. The symmetric kernel function $\mathcal{K}(\cdot)$ is continuously differentiable with bounded derivative on $\mathbb{R}$ satisfying (i) $\mathcal{K}(0) = 1$ and (ii) $|\mathcal{K}(x)| \leq C_6|x|^{-\vartheta}$ as $|x| \to \infty$, for some universal constants $C_6 > 0$ and $\vartheta > 1$.

Condition 4 is commonly used for nonparametric estimation of the long-run covariance matrix; see Newey and West (1987) and Andrews (1991). For kernel functions with bounded support—such as the Parzen kernel and the Bartlett kernel—we have $\vartheta = \infty$ in Condition 4. As indicated in Andrews (1991), to enforce that $\widehat{\Xi}$ given in (12) be positive semi-definite we can require the kernel function $\mathcal{K}(\cdot)$ to satisfy $\int_{-\infty}^{\infty} \mathcal{K}(x)e^{-\iota x\lambda}\,\mathrm{d}x \geq 0$ for any $\lambda \in \mathbb{R}$ with $\iota = \sqrt{-1}$. The Quadratic Spectral, Bartlett, and Parzen kernels all satisfy this requirement.

To construct the parametric bootstrap procedure, let $(\epsilon_1, \ldots, \epsilon_{\tilde{n}})^\top \sim \mathcal{N}(\mathbf{0}, \boldsymbol{\Theta})$ be independent of $\mathcal{X}_n = \{\mathbf{x}_1, \ldots, \mathbf{x}_n\}$, where $\boldsymbol{\Theta}$ is a $\tilde{n} \times \tilde{n}$ matrix with (i,j)th element $\mathcal{K}\{(i-j)/b_n\}$. Following the same arguments in Chang, Yao, and Zhou (2017), conditionally on $\mathcal{X}_n$, we have

$$\frac{1}{\sqrt{\tilde{n}}} \sum_{t=1}^{\tilde{n}} \epsilon_t \hat{\mathbf{c}}_t \sim \mathcal{N}(\mathbf{0}, \widehat{\boldsymbol{\Xi}})$$

with $\widehat{\boldsymbol{\Xi}}$ given in (12). Hence, conditionally on $\mathcal{X}_n$,

$$\hat{\boldsymbol{\eta}}^{\mathrm{ext}}(\omega) := \{\hat{\eta}_1^{\mathrm{ext}}(\omega), \ldots, \hat{\eta}_{2r}^{\mathrm{ext}}(\omega)\}^\top$$

$$= \{\mathbf{I}_r \otimes \mathbf{A}(\omega)\}\left(\frac{1}{\sqrt{\tilde{n}}} \sum_{t=1}^{\tilde{n}} \epsilon_t \hat{\mathbf{c}}_t\right) \qquad (13)$$

is a $(2r)$-dimensional Gaussian process with mean zero and covariance function $\{\mathbf{I}_r \otimes \mathbf{A}(\omega_1)\}\widehat{\boldsymbol{\Xi}}\{\mathbf{I}_r \otimes \mathbf{A}^\top(\omega_2)\}$. Letting

$$\xi_{\mathcal{J}} := \sup_{\omega \in \mathcal{J}} \max_{\ell \in [r]} \{|\hat{\eta}_{2\ell-1}^{\mathrm{ext}}(\omega)|^2 + |\hat{\eta}_{2\ell}^{\mathrm{ext}}(\omega)|^2\}, \qquad (14)$$

our next result shows that the distribution of $\sup_{\omega \in \mathcal{J}} T_n(\omega; \mathcal{I})$ can be approximated by the distribution of $\xi_{\mathcal{J}}$ conditional on $\mathcal{X}_n$.

Proposition 2. Assume Conditions 1–4 hold and $r \geq n^\kappa$ for some sufficiently small constant $\kappa > 0$. Let the bandwidth b_n in (12) satisfy $b_n \asymp n^\rho$ for some constant ρ satisfying $0 < \rho < (\vartheta - 1)/(3\vartheta - 2)$ with ϑ specified in Condition 4. For $\xi_{\mathcal{J}}$ defined in (14), the following two assertions are true as $n \to \infty$.
  (i) If $\mathcal{J} = \{\omega_1, \ldots, \omega_K\}$, then

$$\sup_{u \geq 0} \left|\mathbb{P}\left\{\sup_{\omega \in \mathcal{J}} T_n(\omega; \mathcal{I}) \leq u\right\} - \mathbb{P}(\xi_{\mathcal{J}} \leq u \mid \mathcal{X}_n)\right| = o_{\mathrm{p}}(1)$$

provided that $\log(Kr) \ll f_1(l_n, n; \vartheta, \rho)$, with the bandwidth l_n in (2) satisfying the restriction $\max\{2, C' \log(Kr)\} \leq l_n \ll n^{f_2(\vartheta, \rho)}$

for some sufficiently large constant $C' > 0$, where $f_1(l_n, n; \vartheta, \rho)$ and $f_2(\vartheta, \rho)$ are defined by (21) and (22) in the Appendix, respectively.
  (ii) If $\mathcal{J} = [\omega_L, \omega_U]$, then

$$\sup_{u \geq 0} \left|\mathbb{P}\left\{\sup_{\omega \in \mathcal{J}} T_n(\omega; \mathcal{I}) \leq u\right\} - \mathbb{P}(\xi_{\mathcal{J}} \leq u \mid \mathcal{X}_n)\right| = o_{\mathrm{p}}(1)$$

provided that $\log r \ll f_1(l_n, n; \vartheta, \rho)$, with the bandwidth l_n in (2) satisfying the restriction $\max\{2, C' \log r\} \leq l_n \ll n^{f_2(\vartheta, \rho)}$ for some sufficiently large constant $C' > 0$.

Remark 2. Proposition 2 requires the bandwidth l_n involved in (2) for the estimation of the high-dimensional spectral density matrix $\mathbf{F}(\omega)$ to satisfy the restriction $l_n \ll n^{f_2(\vartheta, \rho)}$. Such a restriction together with $b_n \asymp n^\rho$ is applied to guarantee that the long-run covariance matrix estimate $\widehat{\boldsymbol{\Xi}}$ has a suitable convergence rate to $\boldsymbol{\Xi}$ under the loss $|\cdot|_\infty$. If we select the kernel function $\mathcal{K}(\cdot)$ involved in (12) with bounded support such as the Parzen kernel and the Bartlett kernel, then $\vartheta = \infty$ in Condition 4, which implies l_n should satisfy the restriction $l_n \ll n^{f_2(\infty, \rho)}$ with $f_2(\infty, \rho) = \min\{\rho/3, (1 - 3\rho)/2\}$. Furthermore, letting the bandwidth $l_n \asymp n^\delta$ for some constant $0 < \delta < f_2(\infty, \rho)$ and writing $\tilde{\delta} = \min\{\delta, (\rho - 3\delta)/2, (1 - 3\rho - 2\delta)/8\}$, then Proposition 2(i) holds provided that $\log(Kr) \ll \min\{n^{\tilde{\delta}}, n^{1/9-\delta} \log^{-8/3}(n)\}$, and Proposition 2(ii) holds provided that $\log r \ll \min\{n^{\tilde{\delta}}, n^{1/9-\delta} \log^{-8/3}(n)\}$.

3. Applications

In this section, we present two applications of our established Gaussian approximation theory to inference for the high-dimensional spectral density matrix, including the global hypothesis testing in Section 3.1 and the multiple testing with FDR control in Section 3.2.

3.1. Global Hypothesis Testing

Recall $\mathbf{F}(\cdot) = \{f_{i,j}(\cdot)\}_{p \times p}$. Given $(\mathcal{I}, \mathcal{J})$ such that $\mathcal{I} \subset [p]^2$ with $|\mathcal{I}| = r$ and $\mathcal{J} \subset [-\pi, \pi)$, we consider the following hypothesis testing problem:

$$H_0 : f_{i,j}(\omega) = 0 \text{ for any } (i,j) \in \mathcal{I} \text{ and } \omega \in \mathcal{J} \quad \text{versus}$$
$$H_1 : H_0 \text{ is not true}. \qquad (15)$$

We propose a test statistic for the hypothesis testing problem (15) as follows:

$$T_n = \sup_{\omega \in \mathcal{J}} \max_{(i,j) \in \mathcal{I}} \left|\sqrt{\frac{n}{l_n}} \hat{f}_{i,j}(\omega)\right|^2. \qquad (16)$$

Notice that $T_n = \sup_{\omega \in \mathcal{J}} T_n(\omega; \mathcal{I})$ under the null hypothesis H_0. For given significance level $\alpha \in (0,1)$, based on the theoretical result of Proposition 2 we define the critical value

$$\hat{\mathrm{cv}}_\alpha := \inf\{u > 0 : \mathbb{P}(\xi_{\mathcal{J}} \leq u \mid \mathcal{X}_n) \geq 1 - \alpha\}.$$

Then we reject H_0 specified in (15) at nominal level α if $T_n > \hat{\mathrm{cv}}_\alpha$. Practically, we can always draw $\xi_{\mathcal{J},1}, \ldots, \xi_{\mathcal{J},B}$ independently by (14) for some large integer B, and select the $\lfloor B\alpha \rfloor$th largest value among them as the critical value $\hat{\mathrm{cv}}_\alpha$.

Based on the selection of $\mathcal{J}$, we define

$$M_{\mathcal{J}} = \begin{cases} K, & \text{if } \mathcal{J} = \{\omega_1, \ldots, \omega_K\}, \\ n, & \text{if } \mathcal{J} = [\omega_L, \omega_U]. \end{cases} \quad (17)$$

The next theorem states the theoretical guarantee of our proposed global test.

Theorem 1. Assume Conditions 1–4 hold and $r \geq n^\kappa$ for some sufficiently small constant $\kappa > 0$. Let the bandwidth b_n in (12) satisfy $b_n \asymp n^\rho$ for some constant ρ satisfying $0 < \rho < (\vartheta - 1)/(3\vartheta - 2)$ with ϑ specified in Condition 4, and $\log(M_{\mathcal{J}} r) \ll f_1(l_n, n; \vartheta, \rho)$ with the bandwidth l_n in (2) satisfying $\max\{2, C' \log(M_{\mathcal{J}} r)\} \leq l_n \ll n^{f_2(\vartheta, \rho)}$ for some sufficiently large constant $C' > 0$, where $f_1(l_n, n; \vartheta, \rho)$ and $f_2(\vartheta, \rho)$ are defined as (21) and (22) in the Appendix, respectively. As $n \to \infty$, the following two assertions are true.

(i) Under the null hypothesis H_0, then $\mathbb{P}(T_n > \hat{c}v_\alpha) \to \alpha$.

(ii) Write $\lambda(M_{\mathcal{J}}, r, \alpha) = \{2\log(2M_{\mathcal{J}} r)\}^{1/2} + \{2\log(4/\alpha)\}^{1/2}$ for given $(M_{\mathcal{J}}, r, \alpha)$, and $\varrho = \sup_{\omega \in \mathcal{J}} \max_{\ell \in [2r]} \sigma_\ell^2(\omega)$ with $\sigma_\ell^2(\omega)$ being the ℓth element in the main diagonal of $\Sigma(\omega, \omega)$ defined in (10). Under the alternative hypothesis H_1, then $\mathbb{P}(T_n > \hat{c}v_\alpha) \to 1$ provided that $\sup_{\omega \in \mathcal{J}} \max_{(i,j) \in \mathcal{I}} |f_{i,j}(\omega)| \geq 2n^{-1/2} l_n^{1/2} \varrho^{1/2} \lambda(M_{\mathcal{J}}, r, \alpha)(1 + \epsilon_n)$ for some positive ϵ_n satisfying $\epsilon_n \to 0$ and $\epsilon_n^2 \varrho l_n^{-2} \log^{-2}(l_n) \log^{-1}(n) \lambda(M_{\mathcal{J}}, r, \alpha) \to \infty$.

Theorem 1(i) shows that the size of our proposed global test can maintain the nominal level α asymptotically. Theorem 1(ii) indicates that our proposed global test is consistent under certain local alternatives.

3.2. Multiple Testing with FDR Control

If the global null is rejected, it is important to recover the pairs of indices that correspond to nonzero cross-spectrum (or coherence). That is, we wish to estimate the support of $\mathscr{S}_f$ as in (5). It turns out that support recovery can be formulated as a simultaneous testing problem of $(p^2 - p)/2$ hypotheses $H_{0,i,j}$: $\max_{\omega \in [-\pi, \pi)} |f_{i,j}(\omega)| = 0$ versus $H_{1,i,j}$: $\max_{\omega \in [-\pi, \pi)} |f_{i,j}(\omega)| \neq 0$, for $(i, j) \in [p]^2$ and $i < j$. Below we will present a more general version of the above multiple testing problem. This generality is needed in our real data analysis, where the interest is to recover the support set at the state level based on county-level time series. See Section 5 for details.

Given $\{\mathcal{I}^{(q)}, \mathcal{J}^{(q)}\}$ with $\mathcal{I}^{(q)} \subset [p]^2$ and $\mathcal{J}^{(q)} \subset [-\pi, \pi)$, we consider Q hypothesis testing problems:

$$H_{0,q} : f_{i,j}(\omega) = 0 \text{ for any } (i,j) \in \mathcal{I}^{(q)} \text{ and } \omega \in \mathcal{J}^{(q)} \quad \text{versus}$$
$$H_{1,q} : H_{0,q} \text{ is not true}$$

for $q \in [Q]$. Similar to (16), we propose the test statistic for $H_{0,q}$ as follows:

$$T_n^{(q)} = \sup_{\omega \in \mathcal{J}^{(q)}} \max_{(i,j) \in \mathcal{I}^{(q)}} \left| \sqrt{\frac{n}{l_n}} \hat{f}_{i,j}(\omega) \right|^2,$$

and reject $H_{0,q}$ when $T_n^{(q)}$ takes some large values. Let $\mathcal{H}_0 = \{q \in [Q] : H_{0,q} \text{ is true}\}$ and $\mathcal{H}_1 = \mathcal{H} \setminus \mathcal{H}_0$ denote the sets of true nulls and true alternatives, respectively. Write $Q_0 = |\mathcal{H}_0|$. For each $q \in [Q]$, let $r_q = |\mathcal{I}^{(q)}|$ and $\chi^{(q)}(\cdot) = \{\chi_1^{(q)}(\cdot), \chi_2^{(q)}(\cdot)\}$

be a given bijective mapping from $[r_q]$ to $\mathcal{I}^{(q)}$ such that for any $(i,j) \in \mathcal{I}^{(q)}$, there exists a unique $\ell \in [r_q]$ satisfying $(i,j) = \chi^{(q)}(\ell)$. Analogously, we define a $(2l_n + 1)$-dimensional vector

$$\hat{\mathbf{c}}_{\ell,t}^{(q)} = \frac{1}{2\pi} \big\{ \hat{\hat{x}}_{\chi_1^{(q)}(\ell),t} \hat{\hat{x}}_{\chi_2^{(q)}(\ell),t+l_n} - \hat{\gamma}_{\chi^{(q)}(\ell)}(-l_n), \ldots, $$
$$\hat{\hat{x}}_{\chi_1^{(q)}(\ell),t+2l_n} \hat{\hat{x}}_{\chi_2^{(q)}(\ell),t+l_n} - \hat{\gamma}_{\chi^{(q)}(\ell)}(l_n) \big\}^\top$$

for $\ell \in [r_q]$, where $\hat{\hat{\mathbf{x}}}_t = (\hat{\hat{x}}_{1,t}, \ldots, \hat{\hat{x}}_{p,t})^\top = \mathbf{x}_t - \bar{\mathbf{x}}$. Let $\hat{\mathbf{c}}_t^{(q)} = \{\hat{\mathbf{c}}_{1,t}^{(q),\top}, \ldots, \hat{\mathbf{c}}_{r_q,t}^{(q),\top}\}^\top$ and

$$\hat{\boldsymbol{\eta}}^{\text{ext},(q)}(\omega) := \big\{ \hat{\eta}_1^{\text{ext},(q)}(\omega), \ldots, \hat{\eta}_{2r_q}^{\text{ext},(q)}(\omega) \big\}^\top$$
$$= \{\mathbf{I}_{r_q} \otimes \mathbf{A}(\omega)\} \frac{1}{\sqrt{\tilde{n}}} \sum_{t=1}^{\tilde{n}} \epsilon_t^{(q)} \hat{\mathbf{c}}_t^{(q)},$$

where $\{\epsilon_1^{(q)}, \ldots, \epsilon_{\tilde{n}}^{(q)}\}^\top \sim \mathcal{N}(\mathbf{0}, \Theta)$ and $\mathbf{A}(\omega)$ is defined as (8). Identical to $\hat{\boldsymbol{\eta}}^{\text{ext}}(\omega)$ defined in (13), $\hat{\boldsymbol{\eta}}^{\text{ext},(q)}(\omega)$ is a $(2r_q)$-dimensional Gaussian process with mean zero and covariance function $\{\mathbf{I}_r \otimes \mathbf{A}(\omega_1)\} \widehat{\Xi}^{(q)} \{\mathbf{I}_r \otimes \mathbf{A}^\top(\omega_2)\}$, where $\widehat{\Xi}^{(q)}$ is defined in the same manner of (12) but with replacing $\hat{\mathbf{c}}_t$ by $\hat{\mathbf{c}}_t^{(q)}$. Letting

$$\xi_{\mathcal{J}^{(q)}}^{(q)} := \sup_{\omega \in \mathcal{J}^{(q)}} \max_{\ell \in [r_q]} \big\{ |\hat{\eta}_{2\ell-1}^{\text{ext},(q)}(\omega)|^2 + |\hat{\eta}_{2\ell}^{\text{ext},(q)}(\omega)|^2 \big\},$$

we can show—identical to Proposition 2—that

$$\max_{q \in \mathcal{H}_0} \sup_{u \geq 0} \big| \mathbb{P}\{T_n^{(q)} > u\} - \mathbb{P}\{\xi_{\mathcal{J}^{(q)}}^{(q)} > u \mid \mathcal{X}_n\} \big| = o_{\mathrm{p}}(1). \quad (18)$$

Denote by $\mathrm{pv}^{(q)} = \mathbb{P}\{\xi_{\mathcal{J}^{(q)}}^{(q)} \geq T_n^{(q)} \mid \mathcal{X}_n\}$ and $V_n^{(q)} = \Phi^{-1}\{1 - \mathrm{pv}^{(q)}\}$ the p-value of $H_{0,q}$ and its normal quantile transformation, respectively. For the threshold value t such that $H_{0,q}$ is rejected if $V_n^{(q)} \geq t$, denote the total number of false positives by $R_0(t) = \sum_{q \in \mathcal{H}_0} I\{V_n^{(q)} \geq t\}$, and the total number of rejections by $R(t) = \sum_{q \in \mathcal{H}} I\{V_n^{(q)} \geq t\}$. The false discovery proportion (FDP) and false discovery rate (FDR) are defined, respectively, as

$$\mathrm{FDP}(t) = \frac{R_0(t)}{1 \vee R(t)} \quad \text{and} \quad \mathrm{FDR}(t) = \mathbb{E}\{\mathrm{FDP}(t)\}.$$

Given a prescribed level $\alpha \in (0, 1)$, the key objective for FDR control is to find the smallest $\hat{t}$ such that $\mathrm{FDR}(\hat{t}) \leq \alpha$. To do this, we first consider $\mathrm{FDP}(t)$. Since the true null hypotheses set $\mathcal{H}_0$ is unknown, we need to estimate $R_0(t)$, that is, the numerator of $\mathrm{FDP}(t)$. By (18), it holds that $\mathbb{P}\{V_n^{(q)} \geq t\} = 1 - \Phi(t) + o(1)$ for any $q \in \mathcal{H}_0$. An ideal estimate of $\mathrm{FDP}(t)$ is $\widetilde{\mathrm{FDP}}(t) = Q_0\{1 - \Phi(t)\}/\{1 \vee R(t)\}$. Since Q_0 is unknown, $\widetilde{\mathrm{FDP}}(t)$ is infeasible in practice and we can only estimate $\mathrm{FDP}(t)$ via a more conservative way:

$$\widehat{\mathrm{FDP}}(t) = \frac{Q\{1 - \Phi(t)\}}{1 \vee R(t)}.$$

For given $\alpha \in (0, 1)$, we choose

$$\hat{t} = \inf \big\{ 0 < t \leq (2\log Q - 2\log\log Q)^{1/2} : \widehat{\mathrm{FDP}}(t) \leq \alpha \big\}. \quad (19)$$

If $\hat{t}$ defined in (19) does not exist, let $\hat{t} = (2 \log Q)^{1/2}$. We reject all $H_{0,q}$'s with $V_n^{(q)} \geq \hat{t}$.

To analyze the theoretical properties of our proposed multiple testing procedure, we need to measure the dependency among the marginal test statistics $\{T_n^{(q)}\}_{q \in [Q]}$. Since the limiting distribution of $T_n^{(q)}$ is not pivotal and does not admit an explicit form (or even does not exist), characterization of the dependency among $\{T_n^{(q)}\}_{q \in [Q]}$ is nontrivial. To overcome this difficulty, we consider a transformation of the test statistics $\{T_n^{(q)}\}_{q \in [Q]}$, that is, $\zeta^{(q)} = \Phi^{-1}[F_q\{T_n^{(q)}\}]$, where $\Phi(\cdot)$ and $F_q(\cdot)$ are, respectively, the cumulative distribution functions of the standard normal distribution $\mathcal{N}(0, 1)$, and $T_n^{(q)}$. Due to $\zeta^{(q)} \sim \mathcal{N}(0, 1)$ for each $q \in [Q]$, following Chang et al. (2024b), we can measure the dependency between $T_n^{(q)}$ and $T_n^{(q')}$ by the correlation between $\zeta^{(q)}$ and $\zeta^{(q')}$. It is obvious that the independence between $T_n^{(q)}$ and $T_n^{(q')}$ is equivalent to $\mathrm{Corr}\{\zeta^{(q)}, \zeta^{(q')}\} = 0$. For some constant $\gamma > 0$ and any $q \in [Q]$, define the set

$$\mathcal{S}_q(\gamma) = \left\{ q' \in [Q] : q' \neq q, |\mathrm{Corr}\{\zeta^{(q)}, \zeta^{(q')}\}| \geq \log^{-2-\gamma}(Q) \right\}.$$

For given $q \in [Q]$, the other $Q - 1$ test statistics $\{T_n^{(q')}\}_{q' \in [Q] \setminus \{q\}}$ can be considered in two scenarios: (i) if $q' \in \mathcal{S}_q(\gamma)$, the test statistic $T_n^{(q')}$ has relatively strong dependence with $T_n^{(q)}$, and (ii) if $q' \notin \mathcal{S}_q(\gamma)$, the test statistic $T_n^{(q')}$ has quite weak dependence with $T_n^{(q)}$. To construct the theoretical guarantee of the proposed multiple testing procedure, it is common practice to analyze these two scenarios separately with different technical tools. See also Liu (2013) and Chang, Shao, and Zhou (2016). For each $q \in [Q]$, similar to (17), we define

$$M_{\mathcal{J}^{(q)}} = \begin{cases} K_q, & \text{if } \mathcal{J}^{(q)} = \{\omega_1^{(q)}, \ldots, \omega_{K_q}^{(q)}\}, \\ n, & \text{if } \mathcal{J}^{(q)} = [\omega_L^{(q)}, \omega_U^{(q)}]. \end{cases} \quad (20)$$

Write $M_{\max} = \max_{q \in \mathcal{H}_0} M_{\mathcal{J}^{(q)}}$, $r_{\max} = \max_{q \in \mathcal{H}_0} r_q$ and $r_{\min} = \min_{q \in \mathcal{H}_0} r_q$. Theorem 2 provides the theoretical guarantee of our proposed multiple testing procedure.

Theorem 2. Assume Conditions 1–4 hold, $r_{\min} \geq n^\kappa$ for some sufficiently small constant $\kappa > 0$, and $\max_{1 \leq q \neq q' \leq Q} |\mathrm{Corr} \{\zeta^{(q)}, \zeta^{(q')}\}| \leq r_\zeta$ for some constant $r_\zeta \in (0, 1)$; also assume that $\max_{q \in [Q]} |\mathcal{S}_q(\gamma)| = o(Q^\upsilon)$ for some constants $\gamma > 0$ and $0 < \upsilon < (1 - r_\zeta)/(1 + r_\zeta)$. Let the bandwidth b_n in (12) satisfy $b_n \asymp n^\rho$ for some constant ρ satisfying $0 < \rho < (\vartheta - 1)/(3\vartheta - 2)$ with ϑ specified in Condition 4. If $Q \ll n^{f_3(\vartheta, \rho)}$ for $f_3(\vartheta, \rho)$ defined as (23) in the Appendix, then $\limsup_{n, Q \to \infty} \mathrm{FDR}(\hat{t}) \leq \alpha Q_0/Q$ and $\lim_{n, Q \to \infty} \mathbb{P}\{\mathrm{FDP}(\hat{t}) \leq \alpha Q_0/Q + \varepsilon\} = 1$ for any $\varepsilon > 0$, provided that $\log(M_{\max} r_{\max}) \ll f_4(l_n, n, Q; \vartheta, \rho)$ with the bandwidth l_n in (2) satisfying $\max\{2, C' \log(M_{\max} r_{\max})\} \leq l_n \ll f_5(n, Q; \vartheta, \rho)$ for some sufficiently large constant $C' > 0$, where $f_4(l_n, n, Q; \vartheta, \rho)$ and $f_5(n, Q; \vartheta, \rho)$ are defined as (24) and (25) in the Appendix, respectively.

4. Numerical Simulations

In this section, we investigate the finite sample performance of our proposed methods. The number of parametric bootstrap replications used to determine the critical value $\hat{cv}_\alpha$ in the global testing problem and the p-values in the multiple testing problem is selected as $B = 1000$. We set the sample size to be $n \in \{300, 600\}$, and the dimension to be $p \in \{50, 100, 200\}$, which covers low-, moderate- and high-dimensional scenarios. All reported simulation results in this section are based on 1000 replications.

4.1. Global Hypothesis Testing

Let $\mathcal{I} = \{(i, j) \in [p]^2 : i > j\}$ with $r = |\mathcal{I}| = p(p - 1)/2$. Three types of $\mathcal{J}$ are considered, viz. (i) quarterly seasonal frequencies ($K = 4$) such that $\mathcal{J} = \mathcal{J}^{(4)} = \{-\pi, -\pi/2, 0, \pi/2\}$; (ii) monthly seasonal frequencies ($K = 12$) such that $\mathcal{J} = \mathcal{J}^{(12)} = \{-\pi, -5\pi/6, \ldots, 5\pi/6\}$; (iii) Fourier frequencies ($K = n$) such that $\mathcal{J} = \mathcal{J}^{(n)} = \{-\pi, -(n - 2)\pi/n, -(n - 4)\pi/n, \ldots, (n - 2)\pi/n\}$. Notice that the effective dimension of the parameter we are testing is $p(p - 1)|\mathcal{J}|/2$, which ranges from 4900 (i.e., when $p = 50$ and $\mathcal{J} = \mathcal{J}^{(4)}$) to 11940000 (corresponding to the case $p = 200$ and $\mathcal{J} = \mathcal{J}^{(n)}$ with $n = 600$). For the flat-top kernel (4) involved in (2) for the estimate of the spectral density matrix, we set the constant $c \in \{0.5, 0.8\}$. The associated bandwidths l_n and b_n are determined as stated in Section 2. To examine the empirical size, we consider the following models:

Model 1. Cross-sectionally uncorrelated but dependent sequence: $x_{j,t} = |y_{j-p/10,t}|$ if $j \in \{p/10 + 1, \ldots, p/5\}$ and $x_{j,t} = y_{j,t}$ otherwise, where $\mathbf{y}_t = (y_{1,t}, \ldots, y_{p,t})^\top \overset{\text{iid}}{\sim} \mathcal{N}(\mathbf{0}, a^2 \mathbf{I}_p)$ with $a \in \{0.2, 0.4, 0.6\}$.

Model 2. VAR(1) model: $\mathbf{x}_t = -a\mathbf{x}_{t-1} + \boldsymbol{\varepsilon}_t$ with $\boldsymbol{\varepsilon}_t \overset{\text{iid}}{\sim} \mathcal{N}\{\mathbf{0}, (1 - a^2)\mathbf{I}_p\}$ and $a \in \{0.05, 0.1, 0.2\}$.

Model 3. VMA(1) model: $\mathbf{x}_t = \boldsymbol{\varepsilon}_t - a\boldsymbol{\varepsilon}_{t-1}$ with $\boldsymbol{\varepsilon}_t \overset{\text{iid}}{\sim} \mathcal{N}(\mathbf{0}, \mathbf{I}_p)$ and $a \in \{0.15, 0.2, 0.25\}$.

Model 4. VARMA(2,2) model: $\mathbf{x}_t = \boldsymbol{\Phi}_1 \mathbf{x}_{t-1} + \boldsymbol{\Phi}_2 \mathbf{x}_{t-2} + \boldsymbol{\varepsilon}_t + \boldsymbol{\Theta}_1 \boldsymbol{\varepsilon}_{t-1} + \boldsymbol{\Theta}_2 \boldsymbol{\varepsilon}_{t-2}$, where $\boldsymbol{\varepsilon}_t = (\varepsilon_{1,t}, \ldots, \varepsilon_{p,t})^\top$ with $\varepsilon_{j,t} \overset{\text{iid}}{\sim} t_5$, $\boldsymbol{\Phi}_1 = \mathrm{diag}(0.61\mathbf{1}_{p/2}^\top, 0.41\mathbf{1}_{p/2}^\top)$, $\boldsymbol{\Phi}_2 = 0.15\mathbf{I}_p$, $\boldsymbol{\Theta}_1 = -a \cdot \mathrm{diag}(0.51\mathbf{1}_{p/2}^\top, 0.251\mathbf{1}_{p/2}^\top)$ with $a \in \{0.2, 0.25, 0.3\}$, and $\boldsymbol{\Theta}_2 = -0.05\mathbf{I}_p$.

Due to the lack of competing methods, we only focus on the examination of the performance of our test. As seen from Table 1, our proposed test has relatively accurate sizes when the dimension p is low for Models 1–4. When the sample size n is fixed, the empirical sizes tend to decrease as the dimension p increases, which shows the impact on the parametric bootstrap-based approximation from the dimension p. When the dimension p is fixed, the empirical sizes are closer to the nominal level as the sample size increases from $n = 300$ to $n = 600$. For most settings, the size is below the nominal level and our test is conservative. In settings where our test is over-sized, the amount of over-rejection appears quite mild. So overall the Type-I error is well controlled.

Based on the above size results, we can see that the two choices for c (i.e., $c = 0.5, 0.8$) deliver very similar results, and also our test seems insensitive to K, since setting $K = 4, 12, n$ does not have much impact on the rejection rates.

Table 1. Empirical sizes of the proposed global tests for Models 1–4 at the 5% nominal level based on 1000 repetitions.

			Model 1				Model 2				Model 3				Model 4			
n	p	c	a	$K=4$	$K=12$	$K=n$	a	$K=4$	$K=12$	$K=n$	a	$K=4$	$K=12$	$K=n$	a	$K=4$	$K=12$	$K=n$
300	50	0.5	0.20	2.8	2.8	2.8	0.05	3.5	3.6	3.6	0.15	3.9	3.9	4.0	0.20	4.3	4.8	4.2
			0.40	2.9	2.9	2.7	0.10	4.1	4.1	3.9	0.20	3.8	3.8	3.7	0.25	4.6	5.1	5.0
			0.60	3.0	3.0	2.9	0.20	4.7	4.5	4.2	0.25	3.5	3.8	4.0	0.30	5.5	5.9	5.6
		0.8	0.20	2.9	2.9	2.9	0.05	3.3	3.8	3.3	0.15	4.0	3.9	3.8	0.20	4.9	4.7	4.3
			0.40	2.7	2.8	3.0	0.10	3.8	3.9	4.0	0.20	3.9	3.8	3.8	0.25	4.8	4.8	5.0
			0.60	2.7	3.0	2.9	0.20	4.5	4.7	4.5	0.25	3.6	3.4	3.7	0.30	5.7	5.5	6.0
	100	0.5	0.20	1.7	1.6	1.5	0.05	1.8	2.1	1.9	0.15	2.8	2.8	2.9	0.20	1.9	1.9	1.7
			0.40	1.9	1.8	1.9	0.10	2.7	3.0	3.2	0.20	2.9	2.9	3.1	0.25	2.3	2.4	1.9
			0.60	1.7	1.9	1.9	0.20	3.9	3.2	3.8	0.25	2.6	2.7	2.8	0.30	2.3	2.7	2.8
		0.8	0.20	1.8	1.7	1.6	0.05	1.9	1.9	1.9	0.15	2.7	2.8	2.8	0.20	1.9	2.2	1.9
			0.40	1.7	1.9	2.1	0.10	3.4	3.2	3.4	0.20	2.7	2.7	3.1	0.25	2.0	2.4	2.3
			0.60	1.6	2.1	2.2	0.20	3.5	3.7	3.6	0.25	3.0	3.0	2.5	0.30	2.9	2.7	2.8
	200	0.5	0.20	1.3	1.4	1.4	0.05	1.5	1.9	1.5	0.15	2.0	1.9	1.8	0.20	1.3	1.3	1.2
			0.40	1.1	1.2	1.4	0.10	2.1	1.9	2.0	0.20	1.9	1.8	2.1	0.25	1.5	1.2	1.5
			0.60	1.4	1.1	1.2	0.20	2.3	2.4	2.3	0.25	1.8	1.6	1.8	0.30	1.6	1.6	1.6
		0.8	0.20	1.3	1.5	1.5	0.05	1.5	1.7	1.6	0.15	1.8	1.7	1.8	0.20	1.1	1.2	1.5
			0.40	1.4	1.4	1.5	0.10	2.1	2.0	1.9	0.20	2.2	1.8	1.9	0.25	1.4	1.4	1.5
			0.60	1.3	1.1	1.2	0.20	2.7	2.3	2.5	0.25	1.8	2.0	1.9	0.30	1.5	1.6	1.6
600	50	0.5	0.20	2.7	3.0	3.0	0.05	3.8	3.7	4.1	0.15	4.3	4.3	4.4	0.20	5.9	5.5	5.5
			0.40	2.9	3.1	2.9	0.10	4.4	4.6	4.2	0.20	4.4	4.6	4.6	0.25	6.6	6.2	6.2
			0.60	2.9	3.1	3.0	0.20	4.6	5.3	5.2	0.25	3.8	4.2	4.5	0.30	7.1	7.2	7.2
		0.8	0.20	3.0	3.1	2.9	0.05	3.5	3.8	3.6	0.15	4.4	4.5	4.4	0.20	5.6	5.8	5.6
			0.40	3.1	2.9	3.1	0.10	4.3	4.4	4.3	0.20	4.3	4.7	4.5	0.25	6.2	6.3	6.6
			0.60	2.7	3.2	2.9	0.20	5.1	4.9	5.2	0.25	4.3	3.9	4.4	0.30	7.2	7.0	6.8
	100	0.5	0.20	2.8	2.6	2.6	0.05	3.0	2.9	3.0	0.15	4.7	4.9	4.3	0.20	3.1	3.1	3.3
			0.40	2.9	2.8	2.6	0.10	4.8	4.3	4.4	0.20	4.7	4.6	4.5	0.25	3.9	4.2	3.8
			0.60	2.6	2.5	2.7	0.20	5.5	5.7	5.5	0.25	4.5	4.4	4.2	0.30	4.6	4.7	5.1
		0.8	0.20	2.9	2.7	2.8	0.05	3.2	2.9	3.3	0.15	4.7	4.5	4.5	0.20	3.4	3.5	3.2
			0.40	2.8	2.7	3.0	0.10	4.4	4.3	4.5	0.20	4.5	4.6	4.6	0.25	3.8	3.9	3.9
			0.60	2.6	2.6	2.5	0.20	5.5	5.7	5.6	0.25	4.8	4.0	4.2	0.30	5.0	4.8	4.8
	200	0.5	0.20	2.8	2.7	2.5	0.05	2.9	2.9	3.1	0.15	3.7	4.2	3.6	0.20	2.2	1.9	2.1
			0.40	2.4	2.8	2.5	0.10	3.8	3.7	3.6	0.20	3.3	4.0	3.7	0.25	2.5	2.0	2.2
			0.60	2.4	2.6	2.7	0.20	4.9	4.6	4.5	0.25	3.9	3.6	3.0	0.30	2.9	2.8	2.7
		0.8	0.20	2.7	2.4	2.8	0.05	3.0	2.6	3.0	0.15	3.8	3.5	4.2	0.20	1.9	1.8	1.9
			0.40	2.5	2.8	3.1	0.10	3.7	3.6	3.9	0.20	3.6	3.5	4.1	0.25	2.4	2.3	2.7
			0.60	2.7	2.9	3.2	0.20	4.6	4.6	4.2	0.25	3.4	3.5	3.8	0.30	2.9	2.7	2.8

NOTE: All numbers reported are multiplied by 100.

To study the empirical power of the proposed method, we consider the following models:

Model 5. $\mathbf{x}_t = \boldsymbol{\Psi}\boldsymbol{\varepsilon}_t$, where $\boldsymbol{\varepsilon}_t \overset{\text{iid}}{\sim} \mathcal{N}(\mathbf{0}, \mathbf{I}_p)$ and $\boldsymbol{\Psi} = (\psi_{k,l})_{p \times p}$ for $\psi_{k,l} = 0.4I(k = l) + aI(|k - l| = 1)$ with $a \in \{0.05, 0.1, 0.15\}$.

Model 6. $\mathbf{x}_t = \boldsymbol{\Psi}\mathbf{x}_{t-1} + \boldsymbol{\varepsilon}_t$, where $\boldsymbol{\varepsilon}_t \overset{\text{iid}}{\sim} \mathcal{N}\{\mathbf{0}, (1 - 0.1^2)\mathbf{I}_p\}$ and $\boldsymbol{\Psi} = (\psi_{k,l})_{p \times p}$ for $\psi_{k,l} = -0.1I(k = l) + aI(|k - l| = 1)$ with $a \in \{0.15, 0.2, 0.25\}$.

Model 7. $\mathbf{x}_t = \boldsymbol{\varepsilon}_t - \boldsymbol{\Psi}\boldsymbol{\varepsilon}_{t-1}$, where $\boldsymbol{\varepsilon}_t \overset{\text{iid}}{\sim} \mathcal{N}(\mathbf{0}, \mathbf{I}_p)$ and $\boldsymbol{\Psi} = (\psi_{k,l})_{p \times p}$ for $\psi_{k,l} = 0.2I(k = l) + aI(|k - l| = 1)$ with $a \in \{0.15, 0.2, 0.25\}$.

Model 8. $\mathbf{x}_t = \boldsymbol{\Phi}_1\mathbf{x}_{t-1} + \boldsymbol{\Phi}_2\mathbf{x}_{t-2} + \boldsymbol{\varepsilon}_t + \boldsymbol{\Theta}_1\boldsymbol{\varepsilon}_{t-1} + \boldsymbol{\Theta}_2\boldsymbol{\varepsilon}_{t-2}$, where $\boldsymbol{\varepsilon}_t = (\varepsilon_{1,t}, \ldots, \varepsilon_{p,t})^\top$ with $\varepsilon_{j,t} \overset{\text{iid}}{\sim} t_5$, $\boldsymbol{\Phi}_1 = (\phi_{1,k,l})_{p \times p}$ with $\text{diag}(\boldsymbol{\Phi}_1) = (0.6\mathbf{1}_{p/2}^\top, 0.4\mathbf{1}_{p/2}^\top)^\top$ and $\phi_{1,k,l} = aI(k - l = 1)$ for $k \neq l$ and $a \in \{0.15, 0.2, 0.25\}$, $\boldsymbol{\Phi}_2 = 0.15\mathbf{I}_p$, $\boldsymbol{\Theta}_1 = -0.25 \cdot \text{diag}(0.5\mathbf{1}_{p/2}^\top, 0.25\mathbf{1}_{p/2}^\top)$, and $\boldsymbol{\Theta}_2 = -0.05\mathbf{I}_p$.

Table 2 shows that the power also appears insensitive to the choices of c and K. As the distance from the null hypothesis increases (e.g., a increases), the empirical power of our proposed test grows rapidly to 1. Moreover, enlarging the sample size n helps to increase the empirical power. Overall, the power performance of our proposed test is consistent with our theory under the alternative.

4.2. Multiple Testing

We divide the $p \times p$ matrix $\mathbf{F}(\omega)$ into a 10×10 block submatrix, that is, $\mathbf{F}(\omega) = \{\mathbf{F}_{i,j}(\omega)\}_{i,j \in [10]}$, where each $\mathbf{F}_{i,j}(\omega)$ is a submatrix of size $(0.1p) \times (0.1p)$. The groups of $\{\mathcal{J}_k\}_{k=1}^K$ are set as follows: (i) when $K = 4$, let $\mathcal{J}_k = \{-\pi + (k - 1)\pi/2\}$ be a set with single element for each $k \in [4]$; (ii) when $K = 12$, let $\mathcal{J}_k = \{-\pi + (k - 1)\pi/6\}$ be a set with single element for each $k \in [12]$; (iii) when $K = n$, let $\mathcal{J}_k = \{-\pi + 2(k - 1)\pi/n\}$ be a set with single element for each $k \in [n]$. For each given $(i, j) \in [10]^2$ with $i \leq j$, we consider K marginal hypothesis testing problems $H_{0,i,j,k} : \mathbf{F}_{i,j}(\omega) = \mathbf{0}$ for any $\omega \in \mathcal{J}_k$ versus $H_{1,i,j,k} : H_{0,i,j,k}$ is not true, for $k \in [K]$. Hence, the total number of the marginal hypothesis testing is $Q = 55K$. Due to the fact that $\mathbf{F}(\omega) = (2\pi)^{-1}\boldsymbol{\Psi}^2$ and $(2\pi)^{-1}(\mathbf{I}_p + \boldsymbol{\Psi}^2 - 2\boldsymbol{\Psi}\cos\omega)$, respectively, in Models 5 and 7, then $Q_0 = |\mathcal{H}_0| = 36K$ in these two model settings. For Model 6, since $\mathbf{x}_t = \sum_{j=0}^\infty \boldsymbol{\Psi}^j\boldsymbol{\varepsilon}_{t-j}$ with $\boldsymbol{\varepsilon}_t \overset{\text{iid}}{\sim} \mathcal{N}\{\mathbf{0}, (1 - 0.1^2)\mathbf{I}_p\}$,

Table 2. Empirical powers of the proposed global tests for Models 5–8 at the 5% nominal level based on 1000 repetitions.

			Model 5				Model 6				Model 7				Model 8			
n	p	c	a	$K=4$	$K=12$	$K=n$	a	$K=4$	$K=12$	$K=n$	a	$K=4$	$K=12$	$K=n$	a	$K=4$	$K=12$	$K=n$
300	50	0.5	0.05	88.3	87.3	87.9	0.15	99.6	99.5	99.4	0.15	94.4	94.3	99.4	0.15	74.9	73.2	73.6
			0.10	100	100	100	0.20	100	100	100	0.20	100	100	100	0.20	96.6	95.7	96.1
			0.15	100	100	100	0.25	100	100	100	0.25	100	100	100	0.25	98.1	97.9	98.3
		0.8	0.05	87.7	88.1	80.6	0.15	99.4	99.3	99.5	0.15	93.9	94.1	94.1	0.15	74.4	72.9	74.0
			0.10	100	100	100	0.20	100	100	100	0.20	100	100	100	0.20	96.0	95.9	95.9
			0.15	100	100	100	0.25	100	100	100	0.25	100	100	100	0.25	97.8	98.2	98.2
	100	0.5	0.05	80.9	81.0	81.1	0.15	99.4	99.3	99.6	0.15	91.9	91.9	91.9	0.15	64.8	63.4	63.7
			0.10	100	100	100	0.20	100	100	100	0.20	100	100	100	0.20	96.0	95.5	95.6
			0.15	100	100	100	0.25	100	100	100	0.25	100	100	100	0.25	97.0	97.2	97.4
		0.8	0.05	80.2	80.1	80.6	0.15	99.2	99.3	99.4	0.15	92.1	91.9	91.9	0.15	64.2	63.7	65.0
			0.10	100	100	100	0.20	100	100	100	0.20	100	100	100	0.20	96.0	95.8	96.1
			0.15	100	100	100	0.25	100	100	100	0.25	100	100	100	0.25	96.9	97.0	97.0
	200	0.5	0.05	74.1	74.4	75.1	0.15	99.1	98.9	99.0	0.15	86.3	86.5	85.9	0.15	46.2	45.3	46.6
			0.10	100	100	100	0.20	100	100	100	0.20	100	100	100	0.20	91.3	91.6	91.5
			0.15	100	100	100	0.25	100	100	100	0.25	100	100	100	0.25	96.2	95.8	95.3
		0.8	0.05	73.8	73.8	74.6	0.15	99.1	98.8	99.0	0.15	86.6	86.1	86.3	0.15	45.5	46.1	46.4
			0.10	100	100	100	0.20	100	100	100	0.20	100	100	100	0.20	91.7	91.7	92.2
			0.15	100	100	100	0.25	100	100	100	0.25	100	100	100	0.25	95.8	95.9	96.4
600	50	0.5	0.05	100	99.9	100	0.15	100	100	100	0.15	100	100	100	0.15	99.3	99.3	99.5
			0.10	100	100	100	0.20	100	100	100	0.20	100	100	100	0.20	99.8	99.8	99.8
			0.15	100	100	100	0.25	100	100	100	0.25	100	100	100	0.25	100	100	100
		0.8	0.05	100	100	100	0.15	100	100	100	0.15	100	100	100	0.15	99.3	99.6	99.4
			0.10	100	100	100	0.20	100	100	100	0.20	100	100	100	0.20	99.7	99.8	99.8
			0.15	100	100	100	0.25	100	100	100	0.25	100	100	100	0.25	100	100	100
	100	0.5	0.05	100	100	100	0.15	100	100	100	0.15	100	100	100	0.15	98.5	98.4	98.1
			0.10	100	100	100	0.20	100	100	100	0.20	100	100	100	0.20	99.4	99.5	99.5
			0.15	100	100	100	0.25	100	100	100	0.25	100	100	100	0.25	99.8	99.7	99.9
		0.8	0.05	100	100	100	0.15	100	100	100	0.15	100	100	100	0.15	98.4	98.6	98.3
			0.10	100	100	100	0.20	100	100	100	0.20	100	100	100	0.20	99.6	99.4	99.5
			0.15	100	100	100	0.25	100	100	100	0.25	100	100	100	0.25	99.7	99.9	99.9
	200	0.5	0.05	100	100	100	0.15	100	100	100	0.15	100	100	100	0.15	97.3	97.1	97.2
			0.10	100	100	100	0.20	100	100	100	0.20	100	100	100	0.20	99.6	99.5	99.5
			0.15	100	100	100	0.25	100	100	100	0.25	100	100	100	0.25	98.6	98.5	98.7
		0.8	0.05	100	100	100	0.15	100	100	100	0.15	100	100	100	0.15	97.2	97.3	97.2
			0.10	100	100	100	0.20	100	100	100	0.20	100	100	100	0.20	99.4	99.5	99.4
			0.15	100	100	100	0.25	100	100	100	0.25	100	100	100	0.25	98.7	98.7	98.8

NOTE: All numbers reported are multiplied by 100.

by Example 11.8.1 in Brockwell and Davis (2006), we have $\mathbf{F}(\omega) = 0.495\pi^{-1}(\mathbf{I}_p - \boldsymbol{\Psi}e^{-\iota\omega})^{-1}\{(\mathbf{I}_p - \boldsymbol{\Psi}e^{\iota\omega})^{-1}\}^\top = 0.495\pi^{-1}(\sum_{j=0}^{\infty}\boldsymbol{\Psi}^j e^{-\iota j\omega})(\sum_{k=0}^{\infty}\boldsymbol{\Psi}^k e^{\iota k\omega})^\top$. For Model 8, letting $\boldsymbol{\Phi}(x) = \mathbf{I}_p - \boldsymbol{\Phi}_1 x - \boldsymbol{\Phi}_2 x^2$ and $\boldsymbol{\Theta}(x) = \mathbf{I}_p + \boldsymbol{\Theta}_1 x + \boldsymbol{\Theta}_2 x^2$, again by Example 11.8.1 in Brockwell and Davis (2006) we have $\mathbf{F}(\omega) = (2\pi)^{-1}\sigma_\varepsilon^2 \boldsymbol{\Phi}^{-1}(e^{-\iota\omega})\boldsymbol{\Theta}(e^{-\iota\omega})\boldsymbol{\Theta}^\top(e^{\iota\omega})\{\boldsymbol{\Phi}^{-1}(e^{\iota\omega})\}^\top$, where σ_ε^2 denotes the variance of $\varepsilon_{j,t}$. Note that $\boldsymbol{\Psi}$ and $\boldsymbol{\Phi}_1$ are banded matrices. We know all the sub-nulls in Models 6 and 8 are false and thus $Q_0 = 0$. Hence, we only consider the performance of our multiple testing procedure in Model 5 with $a \in \{0.05, 0.1, 0.15\}$ and Model 7 with $a \in \{0.2, 0.4, 0.6\}$. As with the global testing procedure, we also use the flat-top kernel and the Quadratic Spectral kernel, respectively, in (2) and (12) with the associated bandwidths l_n and b_n determined in the same manner as those in Section 4.1.

Theorem 2 implies that when n and Q grow to infinity, the FDR should be controlled at the level of $\alpha Q_0/Q$ with high probability, which equals 3.27% in our settings with $\alpha = 5\%$. In the vth simulation replication, we can obtain $\hat{t}_v$ defined as (19). For each $q \in [Q]$, denote by $V_{n,v}^{(q)}$ the normal quantile transformation of the p-value for $H_{0,q}$ in the vth simulation replication. See its definition below (18). Besides the empirical FDR, we also consider the empirical power of the proposed

multiple testing procedure defined as

$$\frac{1}{1000}\sum_{v=1}^{1000}\frac{1}{Q-Q_0}\sum_{q\in\mathcal{H}_1} I\{V_{n,v}^{(q)} > \hat{t}_v\}.$$

As shown in Table 3, the empirical FDR becomes closer to the limit rate 3.27% as n increases, and the proposed multiple testing procedure tends to be more conservative when p becomes larger. On the other hand, the corresponding empirical powers grow quickly as n increases, regardless of the smaller empirical FDR. The results also show that different choices of c have little influence on the empirical FDR and power in the models being examined. The choice of K has little impact on the empirical FDR but appears to have some impact on the power. In particular, when K changes from 4 to 12, there is a notable increase in the empirical powers, while the increase becomes insignificant when comparing $K = 12$ with $K = n$.

5. Real Data Analysis

5.1. Batching County-Level Hires Data

As an illustration of the techniques of this article, we study data on new hires at a national level, obtained from the Quarterly

Table 3. Empirical FDRs and powers of the proposed multiple testing procedure based on 1000 repetitions.

			Model 5							Model 7					
			K = 4		K = 12		K = n			K = 4		K = 12		K = n	
	n	p	a	c = 0.5	c = 0.8	c = 0.5	c = 0.8	c = 0.5	c = 0.8	a	c = 0.5	c = 0.8	c = 0.5	c = 0.8	c = 0.5	c = 0.8
Empirical FDRs	300	50	0.05	1.8	1.8	2.0	1.8	1.9	1.9	0.20	1.7	1.8	1.9	2.0	1.9	2.1
			0.10	2.1	2.1	2.3	2.2	2.2	2.2	0.40	1.8	1.8	2.0	2.1	2.2	2.1
			0.15	2.1	2.1	2.2	2.2	2.2	2.2	0.60	1.9	2.0	2.0	2.2	2.2	2.1
		100	0.05	1.5	1.4	1.3	1.4	1.3	1.3	0.20	1.4	1.4	1.5	1.5	1.5	1.6
			0.10	1.7	1.7	1.6	1.7	1.7	1.6	0.40	1.4	1.6	1.6	1.6	1.6	1.6
			0.15	1.8	1.8	1.7	1.8	1.7	1.7	0.60	1.7	1.6	1.7	1.8	1.7	1.8
		200	0.05	1.2	1.0	1.1	1.0	1.1	1.2	0.20	1.0	0.9	1.0	1.0	1.2	0.9
			0.10	1.6	1.4	1.4	1.3	1.5	1.4	0.40	1.3	1.2	1.3	1.3	1.3	1.2
			0.15	1.4	1.4	1.4	1.3	1.3	1.4	0.60	1.2	1.3	1.4	1.4	1.3	1.4
	600	50	0.05	2.3	2.6	2.4	2.4	2.5	2.4	0.20	2.7	2.7	2.8	2.7	2.7	2.7
			0.10	2.8	2.6	2.6	2.6	2.6	2.6	0.40	2.6	2.7	2.8	2.9	2.9	2.8
			0.15	2.9	2.7	2.8	2.8	2.8	2.7	0.60	2.7	2.7	2.8	2.8	2.7	2.9
		100	0.05	2.5	2.4	2.3	2.3	2.5	2.4	0.20	2.2	2.4	2.4	2.4	2.5	2.3
			0.10	2.4	2.4	2.4	2.5	2.6	2.3	0.40	2.4	2.3	2.4	2.4	2.4	2.3
			0.15	2.5	2.4	2.3	2.3	2.4	2.5	0.60	2.4	2.5	2.6	2.6	2.6	2.7
		200	0.05	2.0	2.1	2.1	2.2	2.1	2.0	0.20	1.8	2.0	2.0	1.9	2.0	2.1
			0.10	2.1	2.1	2.2	2.1	2.0	2.1	0.40	1.9	1.9	1.9	1.9	1.8	1.9
			0.15	2.0	2.0	2.1	2.2	2.2	2.0	0.60	2.2	2.2	2.1	2.1	2.2	2.1
Empirical powers	300	50	0.05	32.4	32.3	42.8	43.1	42.7	42.8	0.20	32.9	32.9	38.7	38.5	38.4	38.4
			0.10	95.5	95.6	96.7	96.8	96.8	96.8	0.40	50.9	51.0	69.8	69.7	72.2	72.0
			0.15	99.6	99.7	99.8	99.9	99.8	99.8	0.60	62.6	62.7	81.2	81.2	83.0	83.1
		100	0.05	21.8	21.8	38.2	38.2	38.1	38.0	0.20	30.5	30.4	36.2	36.3	35.7	36.2
			0.10	91.5	91.5	93.3	93.5	93.4	93.3	0.40	49.2	49.1	66.2	66.3	69.0	68.9
			0.15	99.1	99.1	99.5	99.5	99.6	99.5	0.60	58.3	58.1	77.9	78.0	79.4	79.4
		200	0.05	11.0	10.8	33.1	33.0	33.5	33.2	0.20	28.2	28.2	33.3	33.4	34.1	33.5
			0.10	86.0	86.2	88.5	88.7	88.6	88.4	0.40	46.8	46.8	61.7	61.7	62.0	62.2
			0.15	97.8	97.9	98.8	98.7	98.6	98.7	0.60	53.5	53.5	73.9	73.8	74.2	73.9
	600	50	0.05	83.0	82.8	85.4	85.4	85.1	85.3	0.20	48.6	48.6	64.0	64.1	66.0	66.4
			0.10	100	100	100	100	100	100	0.40	60.3	60.4	83.2	83.2	84.1	84.0
			0.15	100	100	100	100	100	100	0.60	94.0	94.0	97.5	97.5	98.0	98.1
		100	0.05	75.5	75.3	78.8	78.8	79.8	79.3	0.20	46.2	46.1	59.4	59.5	60.4	60.2
			0.10	100	100	100	100	100	100	0.40	56.7	56.7	80.6	80.5	81.2	81.4
			0.15	100	100	100	100	100	100	0.60	88.5	88.5	94.9	94.8	95.4	95.1
		200	0.05	67.6	67.7	71.6	71.7	71.8	71.8	0.20	43.4	43.5	54.9	55.0	56.1	56.3
			0.10	99.3	99.5	99.8	99.8	99.8	99.9	0.40	53.8	53.8	78.3	78.3	79.6	79.5
			0.15	100	100	100	100	100	100	0.60	83.2	83.0	91.9	91.8	93.0	92.5

NOTE: All numbers reported are multiplied by 100.

Workforce Indicators (QWI) of the Longitudinal Employer-Household Dynamics program at the U.S. Census Bureau (Abowd et al. 2009).[1] The quarterly data is available for all counties, and we wish to obtain a classification of the database whereby we associate clusters of time series pertaining to various states, such that they are suitable for joint analysis. The national QWI hires data covers a variable number of years, with some states providing time series going back to 1990 (e.g., Washington), and others (e.g., Massachusetts) only commencing at 2010. For each of 51 states (excluding D.C. but including Puerto Rico) there is a new hires time series for each county. Additional description of the data, along with its relevancy to labor economics, can be found in Hyatt and McElroy (2019).

Given QWI county-level data on new hires, we want to know whether we may analyze the data state-by-state, or whether there is additional time series information to be gleaned by examining relationships across states. For any two states i and

j, with $1 \leq i \neq j \leq 51$, let B_i and B_j denote batches of time series indices corresponding to the counties within a state. Between each pair (i, j), we test whether the cross-spectrum between B_i and B_j is not identically zero, with rejection of the null hypothesis indicating there may be merit in considering both batches in a joint time series model. We restrict ourselves to examining the cross-spectrum between distinct batches of series B_i and B_j, which is in contrast to the simulation of Section 4.2, where one can also test B_i with itself. This latter procedure would investigate each state, inquiring whether the county-level time series of that state should be jointly modeled; instead we focus on whether the county-level time series of two distinct states should be jointly modeled. Since the time series are quarterly, we assess the cross-spectrum at the seasonal frequencies, viz. $\mathcal{J} = \{-\pi, -\pi/2, 0, \pi/2\}$. We apply the global test by taking a supremum over the four seasonal frequencies; we also consider multiple testing with FDR control.

Many of the series exhibit strong trend and seasonal effects, and it is important to ensure that the data is stationary; therefore, we apply either regular differencing or seasonal differencing. Although these operations may over-difference certain series, our theory has no requirement that the spectral density
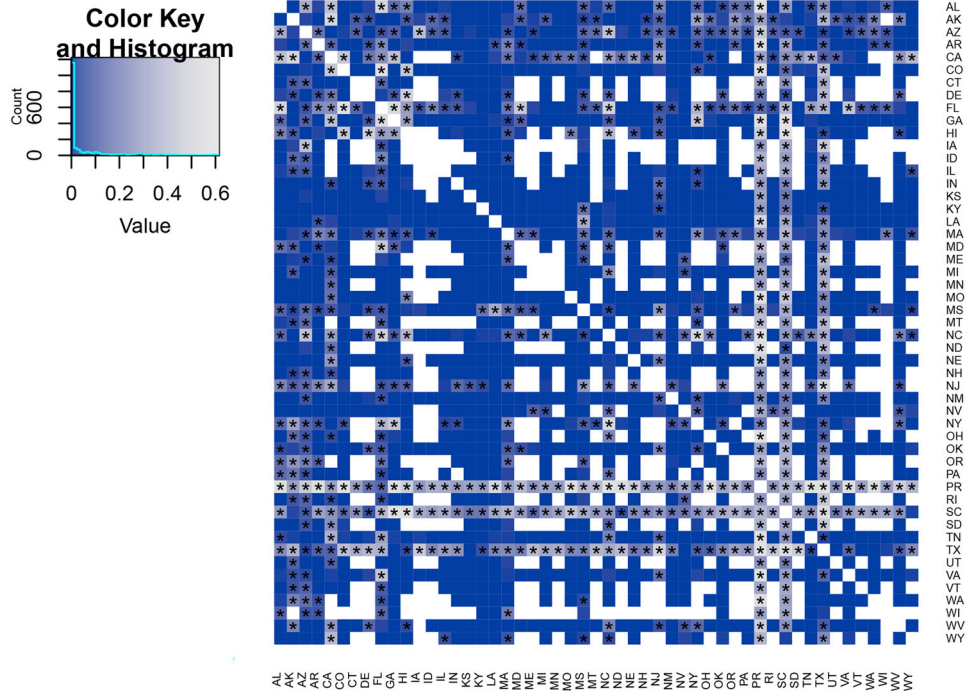
Figure 1. Heatmap of p-values for 51 state pairs, testing whether the cross-spectrum of each pair is zero at seasonal frequencies $\mathcal{J} = \{-\pi, -\pi/2, 0, \pi/2\}$. A white box indicates a pair for which no test is computed; a star marks pairs that are not significant using FDR control, where $\alpha = 5\%$. Each series has been differenced.

be nonzero, so there is no impediment to analysis with this approach. In addition to this data pre-processing, it is necessary to find common sample sizes for each pair of batches B_i and B_j since the start dates differ greatly. In fact, if we were to consider all $p = 3218$ county-level time series in one huge batch, the maximal common sample size is $n = 25$, which is clearly too tiny for such a huge p. Instead, for each of the $\binom{51}{2} = 1275$ possible pairings (B_i, B_j), we determine the common sample available, and the dimension of the resulting paired dataset is $p = |B_i \cup B_j|$. The sample size n in each case is defined to be the most recent contiguous block of times where both batches are fully observed (no missing values); by excluding the sparsely measured counties of Kalawao, HI, and McPherson, NE, we ensure there is a common sample for every pairing. Our methodology requires that $\tilde{n} = n - 2l_n$ (with l_n selected by the data-driven method discussed in Remark 1(c)) is positive; we impose $n > 2l_n + 1$ and $n - d > 7$ (where $d = 1$ for regular differencing and $d = 4$ for seasonal differencing), the latter condition ensuring that the data-driven l_n can be calculated, which ensures $\tilde{n} \geq 2$. For 284 state pairs (or 22.3%) where regular differencing is used the common sample does not meet these requirements, and these cases are skipped over; for the case of seasonal differencing, only 1 state pair violates the requirements.

Our final output is summarized with two heat maps, displayed in Figures 1 and 2, for the cases of regular differencing and seasonal differencing, respectively. Low p-values have a darker color, and most of the pairs end up rejecting the null hypothesis; we have marked with a star those pairs that do not reject the null hypothesis when using the FDR control method with $\alpha = 5\%$. The diagonal, as well as any state pairs with insufficient common sample, is marked white, indicating that no test is conducted in such cases. For the regular differencing there are 338 pairs with no association, and 295 pairs of no association

for the seasonal differencing; hence, there are 653 pairs under regular differencing for which a joint analysis may be useful, and 979 such pairs under seasonal differencing.

5.2. Detecting Seasonal Over-Adjustment in Texas Hires

As a second application of our methods, we focus on the county hires data for Texas, and wish to detect over-adjustment in any of the seasonal adjustments. First we seasonally adjust the data using the automatic methods of the X-13ARIMA-SEATS software (U.S. Census Bureau 2020), excluding Loving county (due to many missing values); note that there is no official seasonal adjustment for these series, and we use default settings in the software so as to eliminate the impact of human intervention in the analysis. We then analyze the $p = 253$ county-level seasonally adjusted time series, testing $H_0 : f_{i,i}(\omega) = 0$ for all $i \in [p]$ with $\mathcal{J} = \{-\pi, -\pi/2, \pi/2\}$, that is, the seasonal frequencies (excluding the trend frequency).

We consider two approaches to the testing: first, we can examine the entire batch of Texan county data by setting $\mathcal{I} = [p]$, thereby obtaining a single test statistic that measures the over-adjustment problem's prevalence for all series. This yields a p-value of 0.203, indicating that at a 5% level there is a failure to reject the null hypothesis of over-adjustment, that is, there is over-adjustment. Second, we can conduct a univariate test for each of the p series, and use the FDR control to manage the multiple testing results. In this case (setting the nominal level at 5%) the support recovery yields 49 counties where the null hypothesis is not rejected; these can then be scrutinized by a human analyst.

This example showcases how the practical problem of seasonally adjusting thousands or millions of time series can be managed with limited computational and human resources: the
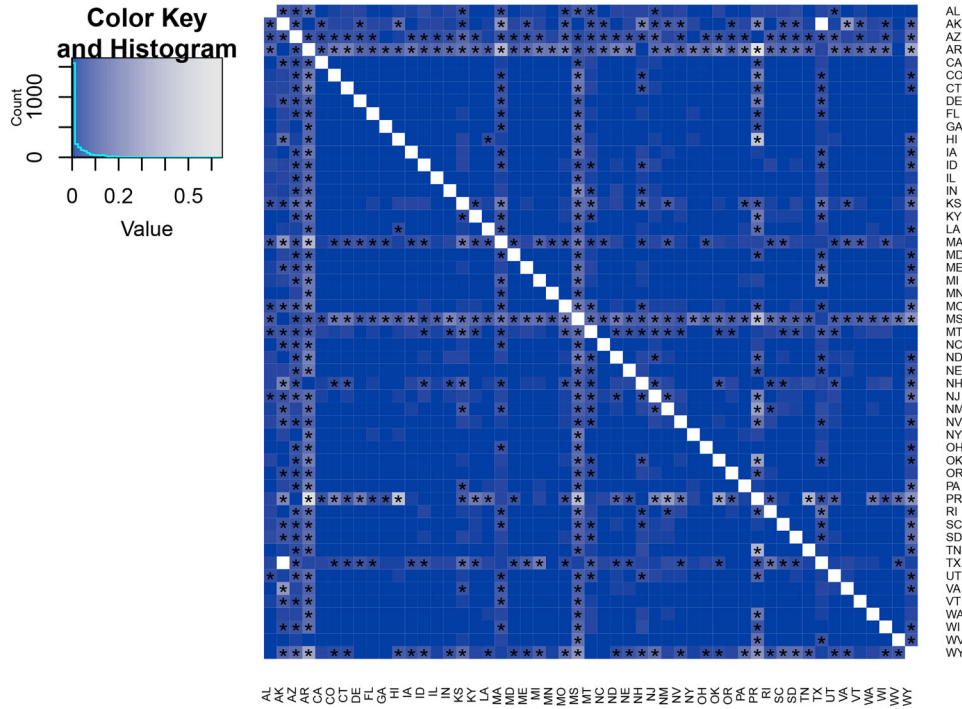
Figure 2. Heatmap of *p*-values for 51 state pairs, testing whether the cross-spectrum of each pair is zero at seasonal frequencies $\mathcal{J} = \{-\pi, -\pi/2, 0, \pi/2\}$. A white box indicates a pair for which no test is computed; a star marks pairs that are not significant using FDR control, where $\alpha = 5\%$. Each series has been seasonally differenced.

automatic methodology of the X-13ARIMA-SEATS software can be applied with default settings, and the output can be quickly assessed for defective adjustments—using FDR control and support recovery, the (hopefully small) subset of problematic seasonal adjustments can then be examined by a seasonal adjustment expert. However, we have not here addressed the more subtle problem of seasonal under-adjustment (where the spectral density of a seasonally adjusted time series still has a local peak at some of the seasonal frequencies), which we leave for future research.

6. Discussion

Motivated by the increasing availability of high-dimensional time series, we develop new inference methodology and theory for the spectral density matrix in the high-dimensional setting, which has not yet been fully explored in the literature. We overcome both methodological and theoretical challenges that high dimensionality induces by extending the celebrated Gaussian approximation and multiplier bootstrap to the testing of a high-dimensional parameter formulated in the frequency domain, which seems to be the first such effort in the literature. In particular, we develop a maximum-type test statistic and computationally feasible parametric bootstrap approximation to test the nullity of coherence at a pre-specified set of frequencies for given component pairs. The theoretical justification is established under a setting that allows weak temporal dependence, flexible contemporary dependence across p components, and exponential rate growth for the dimension. In addition, we develop a multiple testing procedure to recover the support set for the nullity of coherence at a given set of frequencies. A rigorous theory for the FDR control is also provided. Finally,

we illustrate the size and power of the proposed tests through simulations and real data analysis.

Given $\mathcal{I} \subset [p]^2$ and $\mathcal{J} \subset [-\pi, \pi)$, we can also establish the Gaussian approximation theory for

$$\mathcal{T}^{\mathrm{s}} = \sup_{\omega \in \mathcal{J}} \max_{(i,j) \in \mathcal{I}} \left| \sqrt{\frac{n}{l_n}} \frac{\hat{f}_{i,j}(\omega) - f_{i,j}(\omega)}{\{\hat{f}_{i,i}(\omega)\hat{f}_{j,j}(\omega)\}^{1/2}} \right|^2 .$$

Recall $r = |\mathcal{I}|$ and $\tilde{n} = n - 2l_n$. For the bijective mapping $\chi(\cdot) = \{\chi_1(\cdot), \chi_2(\cdot)\}$ specified in Section 2.2, write $\mathbf{W}(\omega) = \mathrm{diag}\{\hat{f}_{\chi_1(1),\chi_1(1)}^{-1/2}(\omega)\hat{f}_{\chi_2(1),\chi_2(1)}^{-1/2}(\omega), \ldots, \hat{f}_{\chi_1(r),\chi_1(r)}^{-1/2}(\omega)\hat{f}_{\chi_2(r),\chi_2(r)}^{-1/2}(\omega)\}$. Letting

$$\xi_{\mathcal{J}}^{\mathrm{s}} = \sup_{\omega \in \mathcal{J}} \max_{\ell \in [r]} \{|\hat{\eta}_{2\ell-1}^{\mathrm{ext,s}}(\omega)|^2 + |\hat{\eta}_{2\ell}^{\mathrm{ext,s}}(\omega)|^2\}$$

with $\{\hat{\eta}_1^{\mathrm{ext,s}}(\omega), \ldots, \hat{\eta}_{2r}^{\mathrm{ext,s}}(\omega)\}^{\top} = \{\mathbf{W}(\omega) \otimes \mathbf{A}(\omega)\}(\tilde{n}^{-1/2} \sum_{t=1}^{\tilde{n}} \epsilon_t \hat{\mathbf{c}}_t)$ for $\mathbf{A}(\omega)$ defined in (8), $\hat{\mathbf{c}}_t = (\hat{\mathbf{c}}_{1,t}^{\top}, \ldots, \hat{\mathbf{c}}_{r,t}^{\top})^{\top}$ with $\hat{\mathbf{c}}_{\ell,t}$ defined in (11), and $(\epsilon_1, \ldots, \epsilon_{\tilde{n}})^{\top} \sim \mathcal{N}(\mathbf{0}, \boldsymbol{\Theta})$ with $\boldsymbol{\Theta}$ defined in Section 2.2, we can show

$$\sup_{u \geq 0} |\mathbb{P}(\mathcal{T}^{\mathrm{s}} \leq u) - \mathbb{P}(\xi_{\mathcal{J}}^{\mathrm{s}} \leq u \,|\, \mathcal{X}_n)| = o_{\mathrm{p}}(1) .$$

Then we can also use the studentized test statistics

$$T_n^{\mathrm{s}} = \sup_{\omega \in \mathcal{J}} \max_{(i,j) \in \mathcal{I}} \left| \sqrt{\frac{n}{l_n}} \frac{\hat{f}_{i,j}(\omega)}{\{\hat{f}_{i,i}(\omega)\hat{f}_{j,j}(\omega)\}^{1/2}} \right|^2 ,$$

$$T_n^{(q),\mathrm{s}} = \sup_{\omega \in \mathcal{J}^{(q)}} \max_{(i,j) \in \mathcal{I}^{(q)}} \left| \sqrt{\frac{n}{l_n}} \frac{\hat{f}_{i,j}(\omega)}{\{\hat{f}_{i,i}(\omega)\hat{f}_{j,j}(\omega)\}^{1/2}} \right|^2$$

in Sections 3.1 and 3.2, respectively, for the associated inference problems. Although T_n^{s} and $T_n^{(q),\mathrm{s}}$ can correct for heterogeneity, their numerical performance is not robust when the sample size

n is small due to the fact that the estimation of the denominator in T_n^{s} and $T_n^{(q),\mathrm{s}}$ may not be accurate enough. Such phenomenon has been empirically observed in Chang et al. (2018). When the sample size n is small, we suggest to use nonstudentized statistics T_n and $T_n^{(q)}$, respectively, for the inference problems considered in Sections 3.1 and 3.2. We can also use the Gaussian approximation technique to construct the simultaneous inference for the coherence matrix. See Section G in the supplementary material for details.

To conclude, we mention several topics that are worth future investigation. First, there are two tuning parameters involved in our procedure, that is, l_n and b_n, the choices of which can have an impact on the finite sample performance. Some theoretical investigation that can lead to a data-driven formula in the high-dimensional setting would be desirable. Andrews' rule for the choice of b_n is used here, but there is no good theoretical justification for it at this moment, and there might be better formulas in practice. Second, as the precision matrix plays an important role for high-dimensional independent and identically distributed data, the partial coherence matrix is the analogue in the spectral domain and its inference in the high-dimensional setting would be of great importance; see Krampe and Paparoditis (2022) for a recent effort. Third, one of the limitations of the spectral density matrix is that it can only characterize second-order properties. Recently, Barunik and Kley (2019) proposed quantile coherency to characterize the cross-series nonlinear dependence in the frequency domain, as an extension of quantile spectrum for univariate time series developed in Hagemann (2013) and Kley et al. (2016). It would be interesting to extend our results to detect nonlinear dependence in the frequency domain for high-dimensional time series. We leave these topics for future research.

Appendix

For given (ϑ, ρ) such that $\vartheta > 1$ and $0 < \rho < (\vartheta - 1)/(3\vartheta - 2)$, let

$$f_1(l_n, n; \vartheta, \rho) := \min \left\{ \frac{n^{\rho/2}}{l_n^{3/2}}, \frac{n^{(1-2\rho)/5}}{l_n^{2/5}}, \frac{n^{(\vartheta+2\rho-3\rho\vartheta-1)/(8\vartheta-4)}}{l_n^{1/4}}, \right.$$
$$\frac{n^{(2\vartheta+3\rho-4\rho\vartheta-2)/(12\vartheta-6)}}{l_n^{1/6}}, \tag{21}$$
$$\left. \frac{n^{1/9}}{l_n \log^{8/3}(l_n)} \right\},$$

$$f_2(\vartheta, \rho) := \min \left(\frac{\rho}{3}, \frac{\vartheta + 2\rho - 3\rho\vartheta - 1}{2\vartheta - 1} \right), \tag{22}$$

$$f_3(\vartheta, \rho) := \min \left(\frac{\rho}{6}, \frac{1-2\rho}{12}, \frac{\vartheta + 2\rho - 3\rho\vartheta - 1}{12\vartheta - 6} \right), \tag{23}$$

$$f_4(l_n, n, Q; \vartheta, \rho) := \min \left\{ \frac{n^{1/9}}{l_n \log^{2/3}(l_n) Q^2}, \frac{n^{(\vartheta+2\rho-3\rho\vartheta-1)/(8\vartheta-4)}}{l_n^{1/4} Q^{3/2}}, \right.$$
$$\frac{n^{(1-2\rho)/5}}{l_n^{2/5} Q^{12/5}}, \tag{24}$$
$$\left. \frac{n^{(2\vartheta+3\rho-4\rho\vartheta-2)/(12\vartheta-6)}}{l_n^{1/6} Q}, \frac{n^{\rho/2}}{l_n^{3/2} Q^3}, \right.$$

$$\left. \frac{n^{1/9}}{l_n \log^{8/3}(l_n)}, \frac{n^{\rho/3}}{Q^2} \right\},$$

$$f_5(n, Q; \vartheta, \rho) := \min \left\{ \frac{n^{(\vartheta+2\rho-3\rho\vartheta-1)/(2\vartheta-1)}}{Q^6}, \frac{n^{\rho/3}}{Q^2} \right\}. \tag{25}$$

Supplementary Materials

The supplementary material contains detailed discussion for Conditions 1–3, all technical proofs of the main results, and the procedure for the statistical inference of high-dimensional coherence matrix.

Acknowledgments

Disclosure Statement

This report is released to inform interested parties of research and to encourage discussion. The views expressed on statistical issues are those of the authors and not those of the U.S. Census Bureau.

Funding

ORCID

Jinyuan Chang 🆔 http://orcid.org/0000-0001-7933-4449

References

Abowd, J. M., Stephens, B. E., Vilhuber, L., Andersson, F., McKinney, K. L., Roemer, M., and Woodcock, S. (2009). "The LEHD Infrastructure Files and the Creation of the Quarterly Workforce Indicators," in *Producer Dynamics: New Evidence from Micro Data*, pp. 149–230, University of Chicago Press. [11]

Andrews, D. W. K. (1991), "Heteroskedasticity and Autocorrelation Consistent Covariance Matrix Estimation," *Econometrica*, 59, 817–858. [5,6]

Barigozzi, M., and Farne, M. (2024), "An Algebraic Estimator for Large Spectral Density Matrices," *Journal of the American Statistical Association*, 119, 498–510. [1]

Barunik, J., and Kley, T. (2019), "Quantile Coherency: A General Measure for Dependence between Cyclical Economic Variables," *The Econometrics Journal*, 22, 131–152. [14]

Bickel, P. J., and Levina, E. (2008), "Covariance Regularization by Thresholding," *The Annals of Statistics*, 36, 2577–2604. [1]

Böhm, H., and von Sachs, R. (2008), "Structural Shrinkage of Nonparametric Spectral Estimators for Multivariate Time Series," *Electronic Journal of Statistics*, 2, 696–721. [1]

——— (2009), "Shrinkage Estimation in the Frequency Domain of Multivariate Time Series," *Journal of Multivariate Analysis*, 100, 913–935. [1]

Bowyer, S. M. (2016), "Coherence a Measure of the Brain Networks: Past and Present," *Neuropsychiatric Electrophysiology*, 2, 1–12. [4]

Brillinger, D. R. (2001), *Time Series*, volume 36 of Classics in Applied Mathematics, Philadelphia, PA: Society for Industrial and Applied Mathematics (SIAM). [1]

Brockwell, P. J., and Davis, R. A. (2006), *Time Series: Theory and Methods*, Springer Series in Statistics, New York: Springer. [1,10]

Cai, T. T., Liu, W., and Luo, X. (2011), "A Constrained l_1 Minimization Approach to Sparse Precision Matrix Estimation," *Journal of the American Statistical Association*, 106, 594–607. [1]

Chang, J., Chen, X., and Wu, M. (2024a), "Central Limit Theorem for High Dimensional Dependent Data," *Bernoulli*, 30, 712–742. [2,5]

Chang, J., He, J., Kang, J., and Wu, M. (2024b), "Statistical Inferences for Complex Dependence of Multimodal Imaging Data," *Journal of the American Statistical Association*, 119, 1486–1499. [8]

Chang, J., He, J., Lin, C., and Yao, Q. (2024c), "HDTSA: An R Package for High-Dimensional Time Series Analysis," arXiv:2412.17341. [3]

Chang, J., Jiang, Q., and Shao, X. (2023), "Testing the Martingale Difference Hypothesis in High Dimension," *Journal of Econometrics*, 235, 972–1000. [2,5,6]

Chang, J., Qiu, Y., Yao, Q., and Zou, T. (2018), "Confidence Regions for Entries of a Large Precision Matrix," *Journal of Econometrics*, 206, 57–82. [14]

Chang, J., Shao, Q.-M., and Zhou, W.-X. (2016), "Cramér-Type Moderate Deviations for Studentized Two-Sample U-Statistics with Applications," *The Annals of Statistics*, 44, 1931–1956. [8]

Chang, J., Yao, Q., and Zhou, W. (2017), "Testing for High-Dimensional White Noise Using Maximum Cross Correlations," *Biometrika*, 104, 111–127. [6]

Chen, X. (2018), "Gaussian and Bootstrap Approximations for High-Dimensional U-Statistics and their Applications," *The Annals of Statistics*, 46, 642–678. [2]

Chen, X., and Kato, K. (2019), "Randomized Incomplete U-Statistics in High Dimensions," *The Annals of Statistics*, 47, 3127–3156. [2]

Chernozhukov, V., Chetverikov, D., and Kato, K. (2013). Gaussian Approximations and Multiplier Bootstrap for Maxima of Sums of High-Dimensional Random Vectors," *The Annals of Statistics*, 41, 2786–2819. [2]

——— (2014), "Gaussian Approximation of Suprema of Empirical Processes," *The Annals of Statistics*, 42, 1564–1597. [5]

——— (2017), "Central Limit Theorems and Bootstrap in High Dimensions," *The Annals of Probability*, 45, 2309–2352. [2]

——— (2019), "Inference on Causal and Structural Parameters Using Many Moment Inequalities," *The Review of Economic Studies*, 86, 1867–1900. [2]

Chernozhukov, V., Chetverikov, D., Kato, K., and Koike, Y. (2022), "Improved Central Limit Theorem and Bootstrap Approximations in High Dimensions," *The Annals of Statistics*, 50, 2562–2586. [2]

——— (2023), "High-Dimensional Data Bootstrap," *Annual Review of Statistics and Its Application*, 10, 427–449. [2]

Eichler, M. (2007), "A Frequency-Domain based Test for Non-Correlation between Stationary Time Series," *Metrika*, 65, 133–157. [1]

Fang, X., and Koike, Y. (2020), "High-Dimensional Central Limit Theorems by Stein's Method," *Annals of Applied Probability*, 31, 1660–1686. [2]

Fiecas, M. B., Leng, C., Liu, W., and Yu, Y. (2019), "Spectral Analysis of High-Dimensional Time Series," *Electronic Journal of Statistics*, 13, 4079–4101. [1]

Fiecas, M. B., and Ombao, H. C. (2011), "The Generalized Shrinkage Estimator for the Analysis of Functional Connectivity of Brain Signals," *The Annals of Applied Statistics*, 5, 1102–1125. [1]

Fiecas, M. B., and von Sachs, R. (2014), "Data-Driven Shrinkage of the Spectral Density Matrix of a High-Dimensional Time Series," *Electronic Journal of Statistics*, 8, 2975–3003. [1]

Forni, M., Hallin, M., Lippi, M., and Reichlin, L. (2000), "The Generalized Dynamic-Factor Model: Identification and Estimation," *The Review of Economics and Statistics*, 82, 540–554. [1]

Hagemann, A. (2013), "Robust Spectral Analysis," SSRN Electronic Journal. [14]

Hall, P. (1991), "On Convergence Rates of Suprema," *Probability Theory and Related Fields*, 89, 447–455. [2]

Hannan, E. J. (1970), *Multiple Time Series*, New York-London-Sydney: Wiley. [1]

Hyatt, H. R., and McElroy, T. S. (2019), "Labor Reallocation, Employment, and Earnings: Vector Autoregression Evidence," *Labour*, 33, 463–487. [11]

Kley, T., Volgushev, S., Dette, H., and Hallin, M. (2016), "Quantile Spectral Processes: Asymptotic Analysis and Inference," *Bernoulli*, 22, 1770–1807. [14]

Krampe, J., and Paparoditis, E. (2022), "Frequency Domain Statistical Inference for High-Dimensional Time Series," arXiv:2206.02250. [2,14]

Liu, W. (2013), "Gaussian Graphical Model Estimation with False Discovery Rate Control," *The Annals of Statistics*, 41, 2948–2978. [8]

Liu, W., and Wu, W. B. (2009), "Asymptotics of Spectral Density Estimates," *Econometric Theory*, 26, 1218–1245. [1]

Loubaton, P., Rosuel, A., and Vallet, P. (2023), "On the Asymptotic Distribution of the Maximum Sample Spectral Coherence of Gaussian Time Series in the High Dimensional Regime," *Journal of Multivariate Analysis*, 194, 105124. [2]

McElroy, T. (2021), "A Diagnostic for Seasonality based Upon Polynomial Roots of ARMA Models," *Journal of Official Statistics*, 37, 367–394. [3]

McElroy, T., and Roy, A. (2022), "A Review of Seasonal Adjustment Diagnostics," *International Statistical Review*, 90, 259–284. [3]

Newey, W., and West, K. D. (1987), "A Simple, Positive Semi-Definite, Heteroskedasticity and Autocorrelation Consistent Covariance Matrix," *Econometrica*, 55, 703–708. [6]

Politis, D. (2003), "Adaptive Bandwidth Choice," *Journal of Nonparametric Statistics*, 15, 517–533. [5]

Politis, D. N. (2011), "High-Order Accurate, Positive Semidefinite Estimation of Large-Sample Covariance and Spectral Density Matrices," *Econometric Theory*, 27, 703–744. [3]

Priestley, M. B. (1981), *Spectral Analysis and Time Series. Vol. 1.* Probability and Mathematical Statistics. Univariate Series. New York and London: Academic Press, Inc. [1,3]

Shao, X. (2009), "A Generalized Portmanteau Test for Independence between Two Stationary Time Series," *Econometric Theory*, 25, 195–210. [1]

Shao, X., and Wu, W. B. (2007), "Asymptotic Spectral Theory for Nonlinear Time Series," *The Annals of Statistics*, 35, 1773–1801. [1]

Sun, F. T., Miller, L. M., and D'Esposito, M. (2004), "Measuring Interregional Functional Connectivity Using Coherence and Partial Coherence Analyses of fMRI Data," *NeuroImage*, 21, 647–658. [4]

Sun, Y., Li, Y., Kuceyeski, A., and Basu, S. (2018), "Large Spectral Density Matrix Estimation by Thresholding," arXiv:1812.00532. [1]

Taniguchi, M., and Kakizawa, Y. (2000), *Asymptotic Theory of Statistical Inference for Time Series*, Springer Series in Statistics, New York: Springer-Verlag. [1]

Tugnait, J. (2022), "On Sparse High-Dimensional Graphical Model Learning for Dependent Time Series," *Signal Processing*, 197, 108539. [1]

U.S. Census Bureau (2020), "X-13ARIMA-SEATS Reference Manual (2020)," https://www2.census.gov/software/x-13arima-seats/x13as/unix-linux/documentation/docx13ashtml.pdf [12]

Wu, W. B., and Zaffaroni, P. (2018), "Asymptotic Theory for Spectral Density Estimates of General Multivariate Time Series," *Econometric Theory*, 34, 1–22. [1]

Yuan, M., and Lin, Y. (2007), "Model Selection and Estimation in the Gaussian Graphical Model," *Biometrika*, 94, 19–35. [1]

Zhang, D., and Wu, W. B. (2017), "Gaussian Approximation for High Dimensional Time Series," *The Annals of Statistics*, 45, 1895–1919. [2]

——— (2021), "Convergence of Covariance and Spectral Density Estimates for High-Dimensional Locally Stationary Processes," *The Annals of Statistics*, 49, 233–254. [1]

Zhang, X., and Cheng, G. (2018), "Gaussian Approximation for High Dimensional Vector Under Physical Dependence," *Bernoulli*, 24, 2640–2675. [2]